Agricultural Systems 201 (2022) 103461

Contents lists available at ScienceDirect

Agricultural Systems

journal homepage: www.elsevier.com/locate/agsy

Quantifying inter-species nitrogen competition in the tomato-corn intercropping system with different spatial arrangements

Ning Chen [a], Xianyue Li [a,c,d,*], Jiří Šimůnek [b], Haibin Shi [a,d], Yuehong Zhang [a], Qi Hu [a]

[a] College of Water Conservancy and Civil Engineering, Inner Mongolia Agricultural University, Huhhot 010018, China
[b] Department of Environmental Sciences, University of California Riverside, Riverside, CA 92521, USA
[c] Collaborative Innovation Center for Integrated Management of Water Resources and Water Environment in the Inner Mongolia Reaches of the Yellow River, Hohhot 010018, China
[d] Research and Development of Efficient Water-saving Technology and Equipment and Research Engineering Center of Soil and Water Environment Effect in Arid Area of Inner Mongolia Autonomous Region, Hohhot 010018, China

HIGHLIGHTS

- The modified HYDRUS-2D model can precisely quantify inter-species nitrogen competition.
- The most intense competition between tomatoes and corn occurred 41–120 days after sowing.
- IC4–2 is the optimal system recommended for sustainable agriculture development.
- *LERN* of the tomato-corn intercropping system decreased with an increase in the planting ratio of tomatoes.

GRAPHICAL ABSTRACT

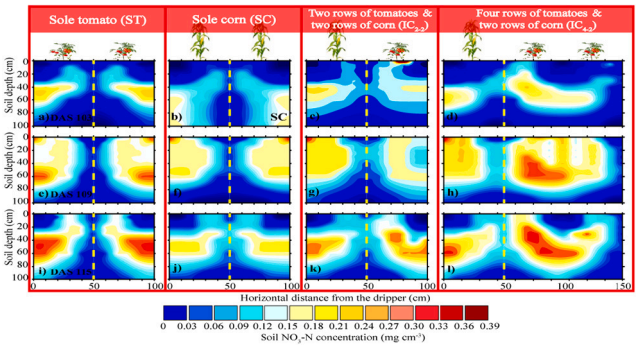

ARTICLE INFO

Keywords:
Inter-species competition
Soil nitrogen dynamic
Intercropping system
Spatial arrangements
HYDRUS (2D/3D)

ABSTRACT

CONTEXT: Intercropping systems have been widely used worldwide due to their high economic benefits and land-use efficiency. While it is well known that inter-species nutrition competition in intercropping systems leads to high production efficiency, the effects of different spatial arrangements of intercropping species on these mechanisms remain unclear.

OBJECTIVE: The objectives of this study were to reveal differences in the soil nitrogen dynamics in the tomato-corn intercropping system with different spatial arrangements of crops and to determine suitable spatial arrangements.

METHODS: A two-year experiment was carried out during the 2018 and 2019 seasons to determine inter-species nitrogen competition in the tomato and corn systems with different spatial arrangements. The treatments included sole corn (SC), sole tomatoes (ST), two rows of tomatoes intercropping two rows of corn (IC_{2-2}), and four rows of tomatoes intercropping two rows of corn (IC_{4-2}) systems. Additionally, the modified HYDRUS (2D/3D) model was used to quantify soil nitrogen concentrations, solute fluxes, soil nitrogen distribution, and soil nitrogen balance in the crop root zone under the SC, ST, IC_{2-2}, and IC_{4-2} systems.

* Corresponding author at: College of Water Conservancy and Civil Engineering, Inner Mongolia Agricultural University, Huhhot 010018, China.
E-mail address: lixianyue80@126.com (X. Li).

https://doi.org/10.1016/j.agsy.2022.103461
Received 11 April 2022; Received in revised form 5 July 2022; Accepted 8 July 2022
Available online 19 July 2022

RESULTS AND CONCLUSIONS: The modified HYDRUS (2D/3D) model could precisely capture the soil nitrogen dynamics with *nRMSE* ranging from 2.8% to 12.4%. In general, soil NH_4-N concentrations in the root zone of tomatoes of different systems decreased as follows: $IC_{2-2} > IC_{4-2} >$ ST, while a reverse trend was observed in the root zone of corn. Compared with soil NH_4-N, differences in soil NO_3-N among different systems were more evident due to its higher mobility. IC_{2-2} had the highest nitrogen flux, cumulative N flux, N uptake (CNU), and the land equivalent ratio for nitrogen (LER_N) among different systems. Among different intercropping systems, the corn's and tomato's highest crop yields occurred in IC_{2-2} and IC_{4-2}, respectively, with an average of 13,406.0 and 98,732.3 kg ha^{-1} in both years. Additionally, corn and tomato's highest nitrogen use efficiency (*NUE*) occurred in IC_{2-2} and ST, respectively. However, the land-equivalent ratio for nitrogen use efficiency (LER_{NUE}) in IC_{4-2} was 5.4% higher than in IC_{2-2}. Therefore, IC_{4-2} is the optimal intercropping system recommended for sustainable agriculture development.

SIGNIFICANCE: The findings of this study improve the understanding of the mechanisms of inter-species nitrogen competition between commercial and grain crops. The study also suggests to the farmers and government suitable spatial arrangements of an intercropping system that can be adopted to promote the development of sustainable agriculture.

1. Introduction

Intercropping has been widely applied worldwide, e.g., in China (Xu et al., 2022), Iran (Firouzi et al., 2017), Brazil (De Conti et al., 2019), and Germany (Nelson et al., 2021). It can effectively optimize plantation structure (Morugán-Coronado et al., 2020), and improve land use efficiency (Latati et al., 2019). In China, especially in the Northwest and South of China, intercropping systems are often used to improve agricultural production (Li, 2016). Intercropping systems improve water use efficiency, nitrogen use efficiency, and field productivity compared with sole crop systems (Coll et al., 2012; Daryanto et al., 2020; Drakopoulos et al., 2021; Jensen et al., 2020; Salehi et al., 2018). In recent years, intercropping systems using commercial crops, e.g., the tomato-corn intercropping system, have become more popular because of increasing economic benefits and controlling soil heavy metal pollution (Salgado et al., 2021; Upadhyay et al., 2010; van Asten et al., 2011). It was reported that the net benefit of producing in the tomato-corn intercropping system could increase by 3467 and 5341 $ ha^{-1} compared with the sole corn and sole tomato systems, respectively (Upadhyay et al., 2010). Moreover, the tomato-corn intercropping system has been shown to effectively decrease the Cd content in the rhizosphere soil by 4.7% and 2.1% compared with the sole tomato and sole corn systems, respectively (Wan et al., 2020). Therefore, it is of great significance to study the tomato-corn intercropping system to increase farmers' income and protect the agricultural ecosystem.

As an essential nutrient substance, nitrogen plays a crucial role in crop growth (Gaudinier et al., 2018). A reasonable nitrogen application strategy can effectively improve crop growth and agricultural production (Groenveld et al., 2021). However, the nitrogen application strategy is hard to formulate for inter-species of the intercropping system because of the complicated inter-species competitive relationships. For example, intensive inter-species competition for nitrogen occurs when soil nitrogen concentrations in the crop root zone cannot meet crop growth needs (for low nitrogen application conditions). Depending on its stronger root uptake ability, the dominant species uptakes soil nitrogen from the root zone of the subordinate species to meet its crop growth. However, subordinate species' growth will be limited due to decreasing soil nitrogen concentrations in the root zone (Dua et al., 2016; Nassab et al., 2011; Zhang and Li, 2003). Although the growth and development of both intercropping species can be promoted in high nitrogen application conditions, this may cause serious non-point source pollution (Manevski et al., 2014). Particularly soil nitrogen from the root zone of the subordinate species can be easily leached due to its greater concentration gradient (Chen et al., 2020a). Therefore, a reasonable nitrogen application strategy needs to be developed by determining the inter-species nitrogen competition relationship in the intercropping system.

Differences in inter-species nitrogen competition exist in different intercropping systems (Ghosh et al., 2009; Galanopoulou et al., 2019; Maitra et al., 2021). In the Gramineaex-Solanaceae (*Lycopersicon esculentum Miller*) intercropping system, although the atmosphere's molecular nitrogen was not transformed to soil ammonium nitrogen to promote crop nitrogen uptake, nitrogen uptake of the dominant species increased by restraining nitrogen uptake of the subordinate species (Long et al., 2021; Zhang et al., 2016). For example, intercropped wheat increased nitrogen uptake by 54.5–375% compared with sole wheat, while nitrogen uptake of intercropped corn decreased by 38.3–42.2% compared with sole corn (Liu et al., 2015). However, research on nitrogen competition between commercial and grain crops is limited.

It is essential to optimize spatial plant arrangements to take advantage of competitive relationships in the intercropping system and achieve maximum economic benefits. Currently, the traditional intercropping system usually involves one crop row intercropping another crop row (Gitari et al., 2020), one crop row intercropping two rows of another crop (Unay et al., 2021), or two crop rows intercropping two rows of another crop (Galanopoulou et al., 2019). Different spatial arrangements of various cultivation crops will result in different soil nitrogen distributions, crop nitrogen uptakes, and nitrogen use efficiencies. Chen et al. (2020a) reported that soil nitrate was distributed mainly in the root zone of tomatoes in the system with two rows of tomatoes intercropping two rows of corn (IC_{2-2}). Choudhary and Choudhury (2016) illustrated that the CNU in the system with one row of corn intercropping five rows of soybeans (IC_{1-5}) was higher than that in the IC_{1-2} system or in the sole crop system.

Although the nitrogen movement, nitrogen redistribution, and nitrogen competition in the root zone of the corn-tomato intercropping system were studied by Chen et al. (2020a), they only focused on nitrogen competition in one type of the intercropping system (i.e., IC_{2-2}). However, soil nitrogen dynamics and competition may differ in different intercropping systems. Various spatial arrangements of tomatoes and corn may alter the nitrogen movement and distribution in the soil profile and affect the competitive nitrogen relationship between intercropping species. Understanding the mechanisms of nitrogen competition in different tomato-corn intercropping systems and determining the suitable spatial arrangements are essential for decreasing non-point pollution and promoting the development of sustainable agriculture.

The numerical model HYDRUS (2D/3D) (Šimůnek et al., 2016) can accurately capture the dynamics of soil water, nitrogen, and salts in complex subsurface systems due to its flexible boundary conditions (e.g., Filipovic et al., 2014; Grecco et al., 2019; Rai et al., 2019). However, the standard HYDRUS (2D/3D) model only considers one vegetation and one set of root water uptake parameters, and it cannot distinguish between root water and nitrogen uptakes by different crops in an intercropping system (Li et al., 2015). Thus, a modified version of HYDRUS (2D/3D) was developed to describe inter-species competition for water and nutrient resources in an intercropping system by considering two sets of root water uptake parameters for two vegetation (Šimůnek et al., 2016). This modified model is used in this study to quantify differences in nitrogen movement, nitrogen distributions, and nitrogen competitive

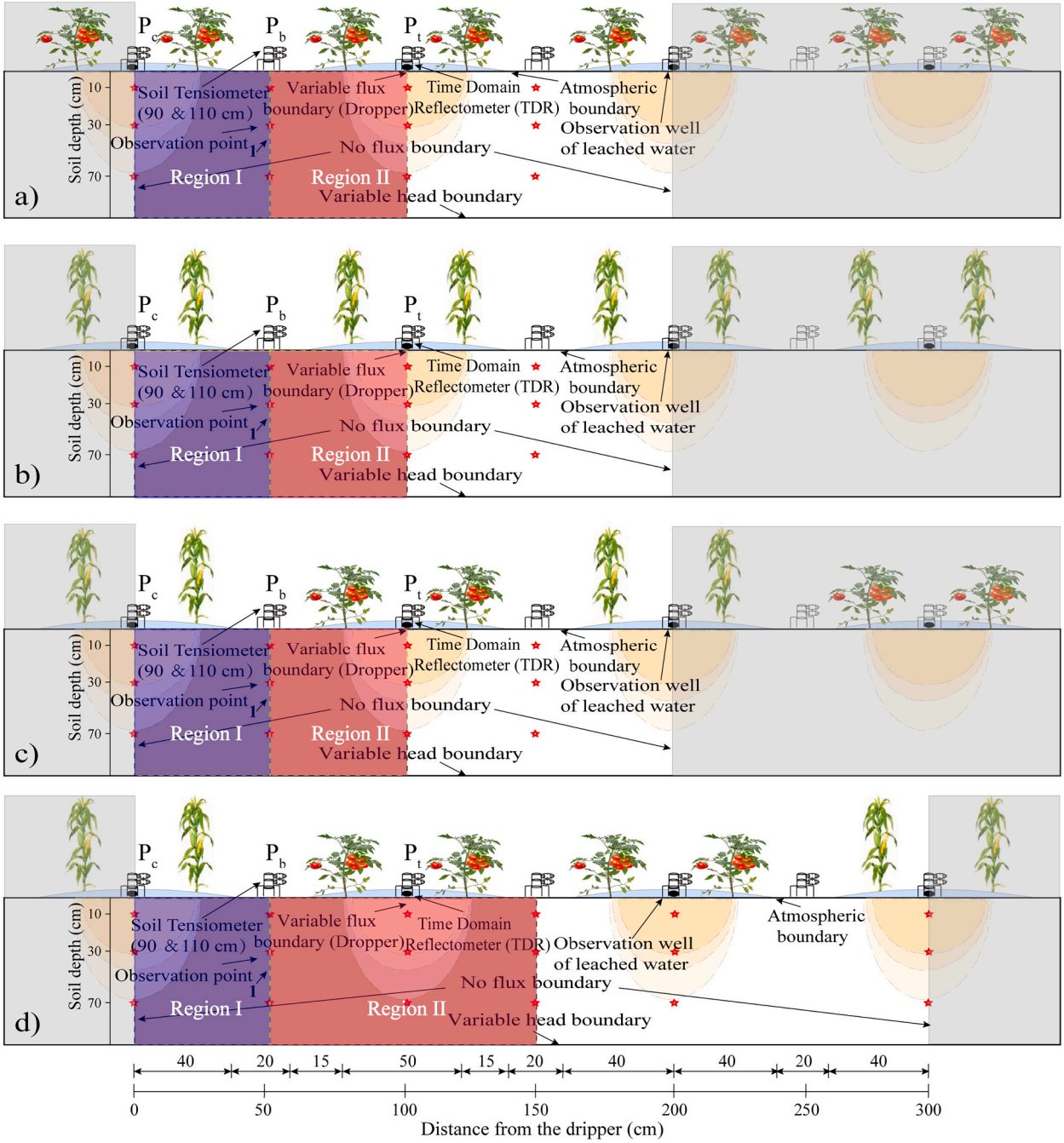

Fig. 1. The modeling domain (unshaded region), boundary conditions, and the planting pattern for the ST (a), SC (b), IC_{2-2} (c), and IC_{4-2} (d) systems. Points P_c, P_b, and P_t are located in the middle between corn rows, between corn and tomato rows, and between tomato rows, respectively.

relationship in the tomato-corn intercropping system with different spatial crop arrangements.

The main objectives of this study are i) to calibrate and validate modified HYDRUS (2D/3D) using observed soil NH_4-N and NO_3-N concentrations, ii) to reveal differences in soil NH_4-N and NO_3-N distributions in the soil profile, iii) to quantify nitrogen fluxes between the root zones of tomatoes and corn, iv) to analyze the nitrogen balance and nitrogen use efficiency in the root zones of tomatoes and corn for different spatial crop arrangements, and v) to compare the competitive ratio for nitrogen and the land equivalent ratio for nitrogen in different systems by scenario simulation.

2. Materials and methods

2.1. Site description

The experiment was conducted at the Jiuzhuang experimental station (40°41′N, 107°18′E; 1041 m above sea level) in the Hetao Irrigation Area, Inner Mongolia, China. This site is located in an arid agro-ecological zone with little annual precipitation (144 mm), high evapotranspiration (593.7 mm), and moderate air temperature (21.2 °C). Soil texture was classified as a silty sand loam with 7% of sand, 89% of silt, and 4% of clay (United States Department of Agriculture, 2010). The soil is moderately alkaline with an average pH of 7.6, organic carbon of 12.1 g kg^{-1}, available nitrogen of 1.0 g kg^{-1}, available phosphorous of 0.8 g

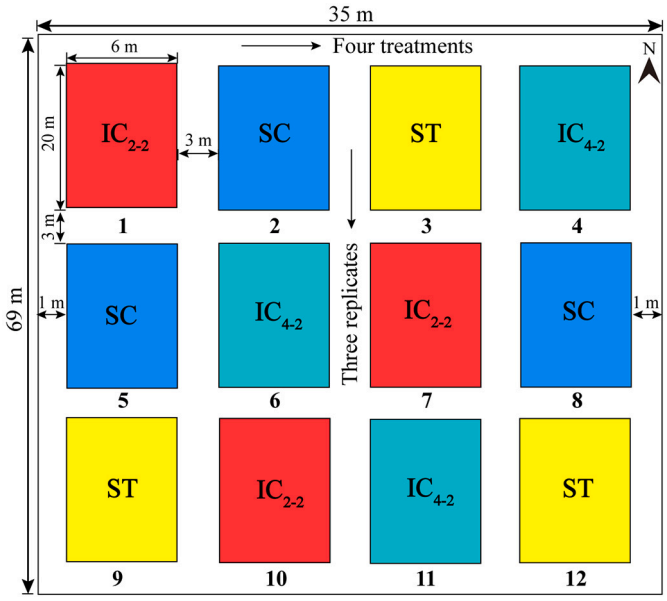

Fig. 2. Schematic of the four experimental treatments (ST, SC, IC_{2-2}, and IC_{4-2}) with three replicates (12 plots).

kg^{-1}, and available potassium of 17.0 g kg^{-1} in the 0–30 m horizons. The soil's bulk density and field capacity in the surface soil layer (0–15 cm) were 1.28 g cm^{-3} and 0.30 cm^3cm^{-3}, respectively.

2.2. On-farm trials and trial management

Corn seeds were sown on May 1, 2018, and May 4, 2019, while tomatoes were transplanted from the greenhouse on May 20, 2018, and May 18, 2019. Local cultivars of corn (*Zea mays L*, cv. Junkai 918) and tomatoes (*Lycopersicon esculentum Miller*, cv. Dunhe 47) were used in the experiment. Experimental treatments consisted of four planting structures: sole corn (SC), sole tomatoes (ST), two rows of tomatoes intercropping two rows of corn (IC_{2-2}), and four rows of tomatoes intercropping two rows of corn (IC_{4-2}) (Fig. 1). The experimental design was a completely randomized design with three replications (Fig. 2). Row spacing (50 cm) and crop spacing (30 cm) were identical in different intercropping systems. Typical local planting densities for corn and tomato were adopted in this study. Moreover, to obtain higher NUE and economic benefits for the tomato-corn intercropping system, this study further increased the planting densities of tomatoes based on the IC_{2-2} system. Planting densities of corn in the sole crop, IC_{2-2}, and IC_{4-2} systems were 60,030, 33,367, and 22,233 seeds ha^{-1}, respectively, while planting densities of tomatoes were 60,030, 33,367, and 44,489 seeds ha^{-1}, respectively. The plot area was 6 m wide and 20 m long, while a 3 m buffer zone separated the plots. To precisely capture the inter-species competition for nitrogen during different crop stages, the entire crop growing season was divided into three growth stages: the first stage (DAS 0–40, i.e., slow NO_3-N exchange), the second stage (DAS 41–120, i.e., intensive NO_3-N exchange), and the third stage (DAS 121–140, i.e., stable NO_3-N exchange). Moreover, three typical days, including one day (DAS 103), seven days (DAS 109), and fourteen days (DAS 115) after the nitrogen fertilizer application, were chosen in the second stage to explore the differences in soil nitrogen distributions in different intercropping systems.

At sowing, 120 kg ha^{-1} of diammonium phosphate and potassium sulphate were uniformly applied to all treatments. Additionally, 210 kg ha^{-1} of urea were applied as topdressing to corn during the crop growing season. 63, 84, and 63 kg ha^{-1} were applied on DAS 47, 81, and 102 in 2018, respectively, while the same application amounts were applied on DAS 44, 75, and 109 in 2019. Moreover, 150 kg ha^{-1} of urea were applied as topdressing to tomatoes during the crop growing season, of which 45, 60, and 45 kg ha^{-1} were applied in different crop stages. The specific fertilization dates for tomatoes were identical to corn. One drip line was installed between two crop rows, with the emitter spacing of 30 cm, the emitter discharge of 2.4 L h^{-1}, and the working pressure of 50–100 kPa. The irrigation uniformity and efficiency of the drip irrigation system were 98% and 95%, respectively. Two valve and water meter (with a precision of 0.001 m^3) groups were installed on drip lines to control and monitor water flow on the tomato and corn sides, respectively. The local recommended irrigation depths for a silty sand loam (30 mm for corn and 22.5 mm for tomatoes) were applied every 7–15 days (Chen et al., 2022). Moreover, the plastic film (with 0.01 mm thickness and 80 cm width) was used in each plot, with the fraction of soil covered by plastic film mulching of 0.8 (Fig. 1).

2.3. Sample collection and analysis

The soil water content (SWC) was determined by three TIME probes (IMKO GmbH Inc.; IPH, TRIME-PICO, Germany) installed in the middle of the corn rows (P_c), middle of the tomato rows (P_t), and in the bare area (P_b). SWCs in 0–20, 20–40, 40–60, 60–80, and 80–100 cm soil depths were observed once every 3–5 days. The probes were calibrated using gravimetric measurements (according to Topp et al., 1980), resulting in the following calibration equation for TIME probes:

$$\theta_g = 0.998\theta_T + 0.02 \ (R^2 = 0.96) \quad (1)$$

where θ_g is the soil water content obtained by the gravimetric measurement ($cm^3\ cm^{-3}$), and θ_T is the soil water content obtained by TIME probes ($cm^3\ cm^{-3}$).

Soil samples for soil nitrogen (NH_4-N and NO_3-N) were collected using a soil auger 100 cm long once every 10–15 days. Collection locations for soil nitrogen were identical to those for SWC. Soil NH_4-N and NO_3-N concentrations were measured using the spectrophotometric method (GB/T 32737–2016). A dry soil sample of 40 g was added to 200 mL KCl solutions (2 mol L^{-1}) and shaken for one hour in a water bath with a constant temperature of 20 ± 2 °C (Bremner and Keeney, 1965). The collected solution was filtered and mixed with phenol and sodium dichloro isocyanurate. After five hours, the soil NH_4-N concentration was determined by ultraviolet spectrophotometry at 630 nm (Beijing General Instrument Co. LTD., TU-1901, General Instrument, CHN). Also, 1 g of dry soil was placed into the reduction column, and 10 mL of the NH_4Cl solution was added. 0.2 mL of color development reagent was added to the colorimetric tube. The soil NO_3-N concentration was determined by ultraviolet spectrophotometry at 543 nm.

Nitrogen leaching was determined by multiplying the nitrogen concentration of the leaching solution by the corresponding water flux. Water fluxes and soil solutions were measured using self-made field lysimeters and a PVC tube opened at the bottom and installed at a depth of 100 cm below the soil surface before corn seeding (Li et al., 2014).

Crop nitrogen uptake was determined using the semi-micro Kjeldahl method (Bremner and Keeney, 1965). Crop samples (stem, leaves, root, and grain) were kept for 30 min at 105 °C temperature and then conserved at 75 °C temperature in the oven to reach a constant weight. After crushing and sieving, a 0.2 g sample was weighted with a weighing paper and digested with 5 mL of concentrated H_2SO_4. The prepared solution was measured by a flow analyzer (Brown ruby Inc., AA3, SEAL, Germany) to determine the nitrogen content of each organ. Crop nitrogen uptake was calculated using the following equation:

$$NU = \sum_{i=1}^{n} m_i c_i' \quad (2)$$

where *NU* is the crop N uptake (mg), m_i is the dry matter mass of each organ (g), and *c'* is the nitrogen content of each organ (mg g^{-1}).

The leaf areas and plant heights were determined by a leaf area meter

(LI-COR Inc. Li- 3000C, LI, USA) and a tape with a precision of 0.1 cm, respectively. Ten plants of each species from each plot were sampled at physiological maturity to measure corn and tomato yield. Root samples for corn and tomatoes under good growth conditions were measured using root samples collected from a soil transect during each crop growth stage. These samples were collected every 5 cm down to a depth of 50 cm, where higher roots density occurred, and then every 10 cm below the 50-cm depth until no roots were found (Chen et al., 2020a). Root samples were scanned using a root system scan (Reagent Instru.; Perfection 4870photo, Epson, Japan), and the root distribution parameters were determined using the WinRHIZO software.

2.4. Calculations analysis

1) Uptake efficiency (*UE*) (Moll et al., 1982; Ahmad et al., 2008; Hajari et al., 2016; Gao et al., 2018; Fernandez et al., 2022):

$$UE = \frac{NU}{NI} \times 100\% \tag{3}$$

where *NU* is the crop nitrogen uptake (kg ha^{-1}), and *NI* is the nitrogen-fertilizer application amount (kg ha^{-1}).

2) Physiological efficiency (*PE*):

$$PE = \frac{CY}{NU} \times 100\% \tag{4}$$

where *CY* is crop yield (kg ha^{-1}).

3) Nitrogen use efficiency (*NUE*):

$$NUE = \frac{CY}{NI} \times 100\% = UE \times PE \tag{5}$$

4) The land equivalent ratio for nitrogen (LER_N) (Salehi et al., 2018; Szumigalski and Van Acker, 2006; Xu et al., 2020):

$$LER_N = \frac{NU_{IC\text{-}t}}{NU_{SC\text{-}t}} + \frac{NU_{IC\text{-}c}}{NU_{SC\text{-}c}} \tag{6}$$

where $NU_{IC\text{-}t}$ is the nitrogen uptake of tomatoes in an intercropping system, $NU_{SC\text{-}t}$ is the nitrogen uptake of tomatoes in a sole crop system, $NU_{IC\text{-}c}$ is the nitrogen uptake of corn in the intercropping system, and $NU_{SC\text{-}c}$ is the nitrogen uptake of corn in a sole crop system. LER_N is the summation of the partial LER_N of single crops in the intercropping system. Partial LER_N shows the relative competitive abilities of single crops in the intercropping system. Note that $LER_N > 1$ indicates an advantage of the intercropping system, and $LER_N < 1$ indicates a disadvantage of the intercropping system.

5) The land equivalent ratio for nitrogen use efficiency (LER_{NUE}):

$$LER_{NUE} = \frac{NUE_{IC\text{-}t}}{NUE_{SC\text{-}t}} + \frac{NUE_{IC\text{-}c}}{NUE_{SC\text{-}c}} \tag{7}$$

where $NUE_{IC\text{-}t}$ is the nitrogen use efficiency of tomatoes in the intercropping system, $NUE_{SC\text{-}t}$ is the nitrogen use efficiency of tomatoes in the sole crop system, $NUE_{IC\text{-}c}$ is the nitrogen use efficiency of corn in the intercropping system, and $NUE_{SC\text{-}c}$ is the nitrogen use efficiency of corn in the sole crop system.

6) The competitive ratio for nitrogen (*CR*) (Zhang et al., 2016):

$$CR_t = \frac{NU_{IC\text{-}t}}{NU_{IC\text{-}t} + NU_{IC\text{-}c}} \times 100\% \tag{8}$$

$$CR_c = \frac{NU_{IC\text{-}c}}{NU_{IC\text{-}t} + NU_{IC\text{-}c}} \times 100\% \tag{9}$$

where CR_t and CR_c are the competitive ratios for nitrogen for tomatoes and corn in the intercropping system, respectively.

7) Economic benefits

Investment and revenue were considered as the economic benefits. Investments included the cost of fertilizer, seed, irrigation, machine, plastic film, pesticides, and labor:

$$I = I_F + I_S + I_I + I_M + I_{PF} + I_D + I_P + I_L \tag{10}$$

where *I* is the investment sum (\$ ha^{-1}), I_F, I_S, I_I, I_M, I_{PF}, I_D, I_P, and I_L are the costs of fertilizer, seed, irrigation, machine, plastic film, pesticides, and labor (\$), respectively.

Revenue was determined based on crop yield (*Y*) and the local price per unit of yield (P_c):

$$R = Y \times P_c \tag{11}$$

where *R* is the revenue (\$ ha^{-1}), P_c is the local price (\$ t^{-1}). The local price of tomatoes and corn were assumed to be 74.6 and 450 \$ t^{-1}, respectively.

The total investment (*TI*), total revenue (*TR*), and net revenue (*NR*) for various intercropping systems were obtained using the following equations:

$$TI = I_t + I_c \tag{12}$$

$$TR = R_t + R_c \tag{13}$$

$$NR = TR - TI \tag{14}$$

where I_t and I_c are the investments in the tomato and corn intercropping systems (\$ ha^{-1}), respectively, and R_t and R_c are the revenues of the tomato and corn intercropping systems (\$ ha^{-1}), respectively.

2.5. HYDRUS (2D/3D) model

2.5.1. Modeling introduction

A modified HYDRUS (2D/3D) model (Šimůnek et al., 2016) simulating the transient two-dimensional movement of water and solutes in the soil profile was adopted to consider two vegetations and two root water and nutrient uptakes. This model describes water flow and nutrient transport in variably saturated porous media using the Richards and convection-dispersion equations, respectively. The solute transport equation considers the advective-dispersive transport in the liquid phase and diffusion in the gaseous phase. The theoretical part of the model is described in detail in its technical manual (Šimůnek et al., 2016) and Appendix.

Actual root water uptakes of corn and tomatoes in the modified HYDRUS (2D/3D) model are determined by the potential transpiration rate (T_p), the root density function, and the piecewise linear water stress response function proposed by Feddes et al. (1978):

$$S(h) = S_c(h) + S_t(h) = \alpha_c(h) \cdot b_c(x,z) \cdot T_{pc} \cdot L_c + \alpha_t(h) \cdot b_t(x,z) \cdot T_{pt} \cdot L_t \tag{15}$$

where S_c and S_t are the root water uptake terms (cm^3 cm^{-3} day^{-1}) for corn and tomatoes, respectively, T_{pc} and T_{pt} are the potential transpiration rates (cm day^{-1}) for corn and tomatoes, respectively, L_c and L_t are the surface lengths associated with transpiration (cm) of corn and tomatoes, respectively, and $b_c(x,z)$ and $b_t(x,z)$ are root water uptake distribution functions (cm^{-2}) for corn and tomatoes, respectively. T_p was obtained as a fraction of potential evapotranspiration (ET_p) using Beer's law. The root density functions for corn and tomatoes ($b_c(x,z)$ and $b_t(x,z)$, respectively) were calculated based on the actual root distribution.

Table 1
Soil hydraulic parameters (the residual water content, θ_r, the saturated water content, θ_s, the shape parameters, α, n, and l, and the saturated hydraulic conductivity, K_s) and solute transport parameters (the longitudinal dispersivity, D_L, the transverse dispersivity, D_T, the distribution coefficient, K_d, and the molecular diffusion coefficient, λ) of the 0–20 cm, 20–40 cm, and 40–100 cm soil depths. Note that subscripts 1 and 2 represent NH_4-N and NO_3-N, respectively.

Depth (cm)	Soil hydraulic parameters						Solute transport parameters					
	θ_r ($cm^3\ cm^{-3}$)	θ_s ($cm^3\ cm^{-3}$)	α (cm^{-1})	n (−)	K_s ($cm\ day^{-1}$)	l (−)	D_L (cm)	D_T (cm)	K_{d1} ($cm^3\ g^{-1}$)	K_{d2} ($cm^3\ g^{-1}$)	λ_1 ($cm^2\ h^{-1}$)	λ_2 ($cm^2\ h^{-1}$)
0–20	0.053	0.436	0.006	1.63	65.1	0.5	10	1				
20–40	0.050	0.388	0.07	1.61	43.4	0.5	5	0.5	3.5	0	0.064	0.068
40–100	0.044	0.383	0.09	1.55	22.5	0.5	5	0.5				

The root water uptake stress reduction functions for corn and tomatoes ($a_c(h)$ and $a_t(h)$, respectively) can be calculated as follows:

$$\alpha(h) = \begin{cases} \dfrac{h_1 - h}{h_1 - h_2} & h_2 < h \le h_1 \\ 1 & h_3 \le h \le h_2 \\ \dfrac{h - h_4}{h_3 - h_4} & h_4 \le h < h_3 \end{cases} \quad (16)$$

where h_1 is the anaerobic point pressure head (cm), h_2 and h_3 are the pressure heads between which root water uptake is optimal (cm), and h_4 is the wilting point pressure head (cm). The water stress parameters for corn and tomato provided by Wesseling and Brandyk (1985) were adopted in this study, i.e., h_1, h_2, h_3, and h_4 were set at −15, −325, −600, and − 8000 cm for corn, respectively; and − 30, −800, −1500, and − 8000 cm for tomatoes, respectively.

The reactive transport of nitrogen species is considered to be described using a first-order sequential reaction chain, in which NH_4-N first transforms into NO2-N and then further into NO3-N. However, since the transformation from NO_2-N to NO_3-N is significantly faster than the transformation from NH_4-N to NO_2-N, the intermediate species (NO_2-N) can be neglected in the model (Please see Appendix). Additionally, the denitrification, volatilization, immobilization, and mineralization processes were neglected in the model, similarly to many other studies (e.g., Ramos et al., 2012; Tafteh and Sepaskhah, 2012). Chen et al. (2020b) explained the reasons for this simplification in detail. This study further assumed that NO3-N is present only in the dissolved phase, and NH_4-N is linearly distributed between the dissolved and adsorbed phases. Thus, the distribution coefficient (K_d) was set to zero and 3.5 $cm^3\ g^{-1}$ for NO3-N (K_{d2}) and NH_4-N (K_{d1}), respectively (Hanson et al., 2006). Additionally, solute transport parameters, including the longitudinal dispersivity (D_L), the transverse dispersivity (D_T), and the molecular diffusion coefficients, depend mainly on soil texture and solute properties (Table 1). The calibrated longitudinal dispersivity (D_L) was considered 10 cm for 0–20 cm soil layer, 5 cm for 20–40 cm soil layer, and 5 cm for 40–100 cm soil layer. The transverse dispersivity (D_T) was taken as one-tenth of D_L (Cote et al., 2003; Hanson et al., 2006; Ramos et al., 2012). Also, the molecular diffusion coefficients (λ) for NH4-N (λ_1) and NO3-N (λ_2) in free water were set to 0.064 and 0.068 $cm^2\ h^{-1}$, respectively (Cote et al., 2003; Nakamura et al., 2004). Soil hydraulic parameters (including the shape parameters, α and n, and the saturated hydraulic conductivity, K_s) and solute transport parameters (including the longitudinal dispersivity, D_L, and the transverse dispersivity, D_T) were manually adjusted by comparing simulated and observed SWC and soil nitrogen concentration values until a good accuracy was achieved.

Nutrient uptake by roots is associated with root water uptake S, which is computed using the following equations:

$$S_{s1} = S_c(h)c_{c1} + S_t(h)c_{t1} \quad (17)$$

$$S_{s2} = S_c(h)c_{c2} + S_t(h)c_{t2} \quad (18)$$

where subscripts 1 and 2 refer to corn and tomatoes, respectively, S_s is root nutrient uptake ($mg\ cm^{-3}\ d^{-1}$), c_{c1} and c_{t1} are the NH_4-N concentrations taken up by corn and tomatoes roots ($mg\ cm^{-3}$), respectively, and c_{c2} and c_{t2} are the NO_3-N concentrations taken up by corn and tomatoes roots ($mg\ cm^{-3}$), respectively.

2.5.2. Initial and boundary conditions

In the tomato-corn intercropping system, inter-species nitrogen competition was evaluated in a rectangular domain shown in Fig. 1. The transport domain was discretized using 1920 two-dimensional triangular finite elements to ensure a fine spatial discretization of the area close to the soil surface. Measured SWCs were used as the initial conditions in the model. Additionally, the initial conditions for NH_4-N and NO3-N were set to zero due to the soil profile's initially low soil nitrogen concentration. At the soil surface, the time-variable flux and atmospheric boundary conditions (BC) were specified to represent emitters and the soil surface between emitters, respectively. The time-variable BC represented drip irrigation. Since plastic film mulching can effectively cut off the water vapor transport between the soil surface and the atmosphere, the mulched soil surface was assigned a "No Flow" BC. The atmospheric BC includes precipitation, potential evaporation, and potential transpiration fluxes. Potential evaporation and transpiration were obtained as fractions of potential evapotranspiration (ET_p), and ET_p was obtained by multiplying reference evapotranspiration (ET_0) by the crop coefficient (K_c). K_c for corn and tomatoes were taken from the FAO paper (Allen et al., 1998). The extinction coefficients for corn and tomatoes equal 0.39 (Li et al., 2018) and 0.65 (Cruz et al., 2014), respectively.

The emitter water and solute fluxes for a particular boundary were calculated as follows (Chen et al., 2020a):

$$q_c = Q_c / L_c' = I_c \times L_c / L_c' \quad (19)$$

$$q_t = Q_t / L_t' = I_t \times L_t / L_t' \quad (20)$$

$$q_{sc} = q_c \times c_{c0} \quad (21)$$

$$q_{st} = q_t \times c_{t0} \quad (22)$$

where q_c and q_t are the boundary fluxes ($cm\ day^{-1}$) for corn and tomatoes, respectively, Q_c and Q_t are the actual emitter fluxes ($cm^2\ day^{-1}$) for corn and tomatoes, respectively, I_c and I_t are the irrigation depths (mm) for corn and tomatoes, respectively, L_c and L_t are the widths of the canopy (cm) for corn and tomatoes, respectively, L_c' and L_t' are the widths of the variable-flux BC (cm) for corn and tomatoes, respectively, q_{sc} and q_{st} are the solute fluxes across the boundary ($mg\ cm^{-2}\ day^{-1}$) for corn and tomatoes, respectively, and c_{c0} and c_{t0} are the nitrogen concentrations in irrigation water ($mg\ cm^{-3}$) for corn and tomatoes, respectively. In this study, I, L, and L' for corn were 3, 40, and 5 cm, respectively, and 2.25, 40, and 5 cm for tomatoes.

A time-variable pressure head BC was applied along the bottom boundary to represent the effects of the shallow groundwater table on water flow and soil nitrogen dynamics. Additionally, the third-type Cauchy BC was used for solute transport along all boundaries with a specified water flux BC (at the top boundary), while the second-type Neumann BC was used for solute transport along outflow boundaries (at the bottom boundary). Two lateral boundaries of the flow domain were assigned a no-flow BC.

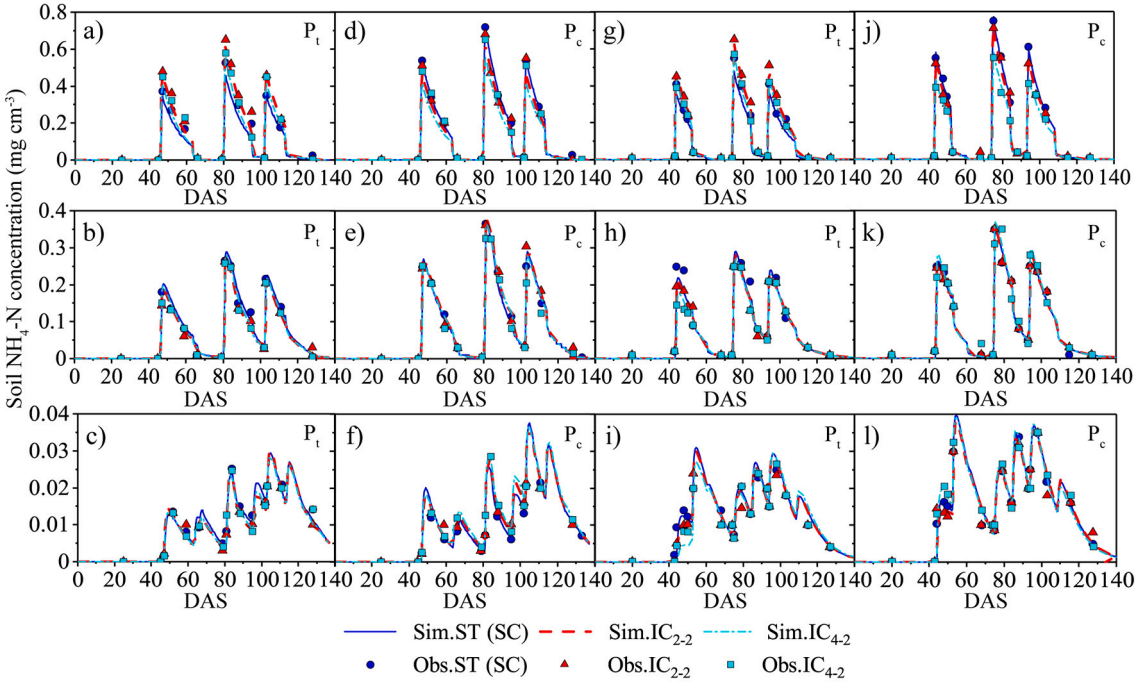

Fig. 3. Observed and simulated soil NH_4-N concentrations in P_c (a, b, c, g, h, i) and P_t (d, e, f, j, k, l) in the 0–20 (top), 20–40 (middle), and 40–100 cm (bottom) soil layers in the ST, SC, $IC_{2–2}$, and $IC_{4–2}$ systems during the 2018 (a-f) and 2019 (g-l) seasons.

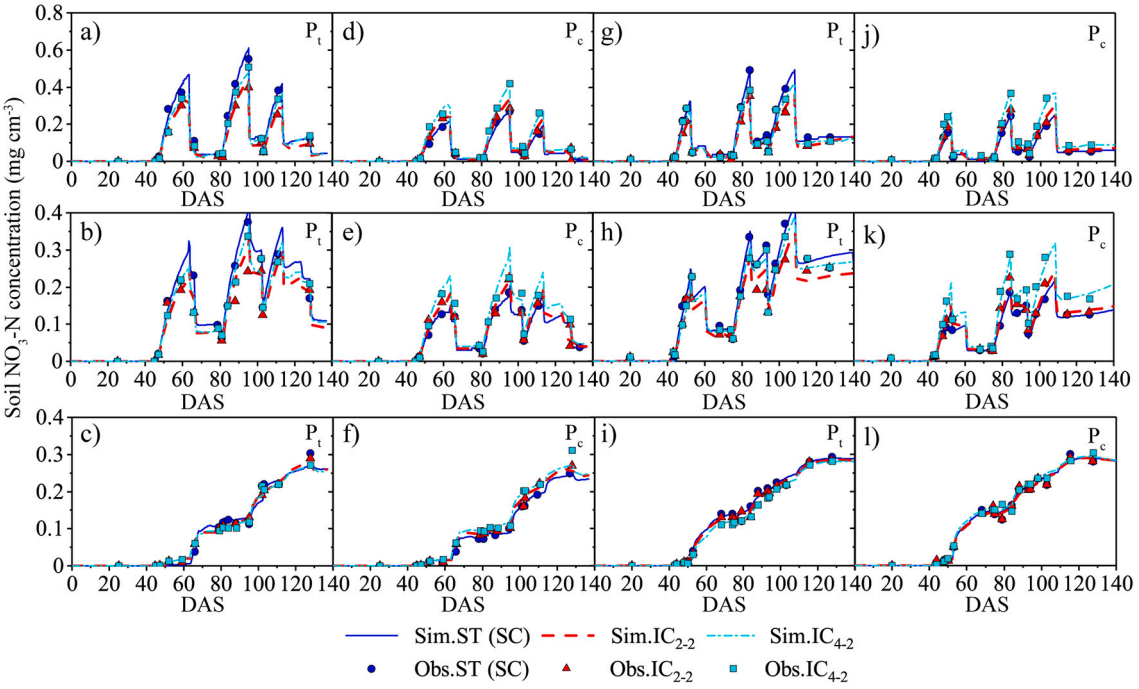

Fig. 4. Observed and simulated soil NO_3-N concentrations in P_c (a, b, c, g, h, i) and P_t (d, e, f, j, k, l) in the 0–20 (top), 20–40 (middle), and 40–100 cm (bottom) soil layers in the ST, SC, $IC_{2–2}$, $IC_{4–2}$ systems during the 2018 (a-f) and 2019 (g-l) seasons.

2.5.3. Scenario analysis

To further assess the mechanisms of the nitrogen competition between tomatoes and corn in different intercropping systems, we carried out seven scenario simulations, i.e., SC, $IC_{2–2}$, $IC_{4–2}$, $IC_{6–2}$, $IC_{8–2}$, $IC_{10–2}$, and ST. Two important indicators (*CR* and LER_N) were used to evaluate the nitrogen competition between tomatoes and corn in different intercropping systems.

2.5.4. Statistical analysis

The statistical difference among different experimental treatments was determined by the analysis of variance (ANOVA) with a significance level of 0.05 using Statistical Product and Service Solutions (SPSS) version 22.0. Moreover, to evaluate the model performance in simulating the NH_4-N and NO3-N fate and transport, the percent bias (*PBIAS*), the index of agreement (*IA*), and the normalized root mean square error (*Nrmse*) were computed in addition to a graphical

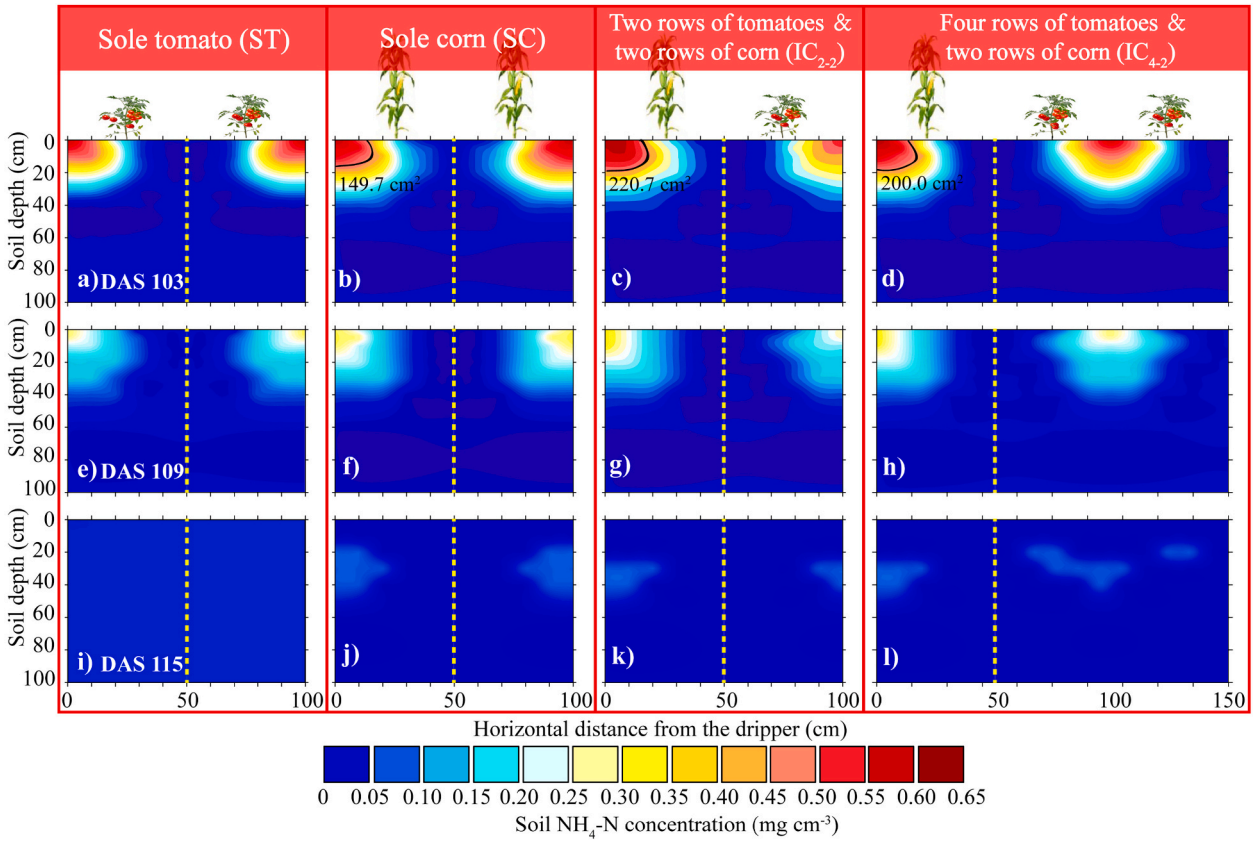

Fig. 5. Simulated two-dimensional distributions of NH_4-N concentrations one day (DAS 103) (top), seven days (DAS 109) (middle), and fourteen days (DAS 115) (bottom) after the nitrogen fertilizer application in the ST (a, e, i), SC (b, f, j), IC_{2-2} (c, g, k), and IC_{4-2} (d, h, l) systems.

comparison of observed and simulated values.

$$PBIAS = \frac{\sum_{i=1}^{n}(O_i - S_i)}{\sum_{i=1}^{n} O_i} \times 100\% \quad (23)$$

$$IA = 1 - \frac{\sum_{i=1}^{n}(S_i - O_i)^2}{\sum_{i=1}^{n}(|S_i - \overline{O}| + |O_i - \overline{O}|)^2} \quad (24)$$

$$nRMSE = \frac{\sqrt{\frac{1}{n}\sum_{i=1}^{n}(S_i - O_i)^2}}{Max(O_i) - Min(O_i)} \times 100\% \quad (25)$$

where S is the simulated value, O is the observed value, $\bar{O}$ is the mean observed value, and n is the number of observed values.

3. Results

3.1. Evaluation of HYDRUS (2D/3D)

The soil NH_4-N and NO_3-N concentrations measured in the root zone in 2018 were used to calibrate the HYDRUS (2D/3D) model parameters, while the corresponding data in 2019 were used to verify the simulation accuracy. The result showed that HYDRUS (2D/3D) could precisely capture the dynamics of soil NH_4-N and soil NO_3-N (Table 1). During the calibration period, the average *PBIAS*, *IA*, and *Nrmse* for soil NH_4-N concentrations in different systems were 2.1%, 0.88, and 7.2%, respectively. The corresponding statistics for soil NO_3-N concentrations were − 2.2%, 0.89, and 7.2%. During the verification period, the average *PBIAS*, *IA*, and *Nrmse* for soil NH_4-N concentrations in different systems were 8.2%, 0.86, and 8.6%, respectively, and the corresponding statistics for soil NO_3-N concentrations were 7.5%, 0.84, and 7.8%. In general, estimation accuracy was good for the ST, SC, IC_{2-2}, and IC_{4-2} systems, with *PBIAS* ranging from −13.3% to 13.5% and *Nrmse* ranging from 2.8% to 12.4%. Additionally, *IA* for soil NH_4-N and NO_3-N concentrations in different systems was above 0.82, indicating that the simulated values agree well with the measured value (Table 1). Therefore, HYDRUS (2D/3D) can be used to evaluate nitrogen competition between corn and tomatoes in different intercropping systems.

Apparent spatial-temporal differences between soil nitrogen concentrations were found between different systems. The largest differences in soil NH_4-N concentrations among different systems occurred in the surface soil layer (0–40 cm), especially in 0–20 cm (Fig. 3). In general, soil NH_4-N concentrations at P_t in different systems decrease as follows: $IC_{2-2} > IC_{4-2} >$ ST. Average soil NH_4-N concentrations at P_t in IC_{2-2} were 19.6% and 10.4% higher than in ST and IC_{4-2}, respectively. Also, the highest soil NH_4-N concentration at P_c in different systems occurred in the SC treatment, increasing by 2.9% and 12.1% compared with IC_{2-2} and IC_{4-2}. However, the highest soil NO_3-N concentrations at P_t and P_c occurred in the ST and IC_{4-2} treatments, respectively (Fig. 4). In the 0–20 cm soil layer, the average soil NO_3-N concentration at P_t in ST increased by 28.5% and 15.7% compared with IC_{2-2} and IC_{4-2}, respectively. The average soil NO_3-N concentration at P_c in IC_{4-2} increased by 33.8% and 23.1% compared to SC and IC_{2-2}, respectively. In the 20–40 cm soil layer, the average soil NO_3-N concentration at P_t in ST was 20.5% and 10.9% higher than in IC_{2-2} and IC_{4-2}, respectively, while the soil NO_3-N concentration at P_c in IC_{4-2} was 29.6% and 22.1% higher than in SC and IC_{2-2}, respectively. In the 40–100 cm soil layer, the average soil NO_3-N concentrations at P_t in ST, IC_{2-2}, and IC_{4-2} were 0.11, 0.11, and 0.10 mg cm^{-3}, respectively, and the soil NO_3-N concentrations at P_c in SC, IC_{2-2}, and IC_{4-2} were 0.10, 0.11, and 0.11 mg

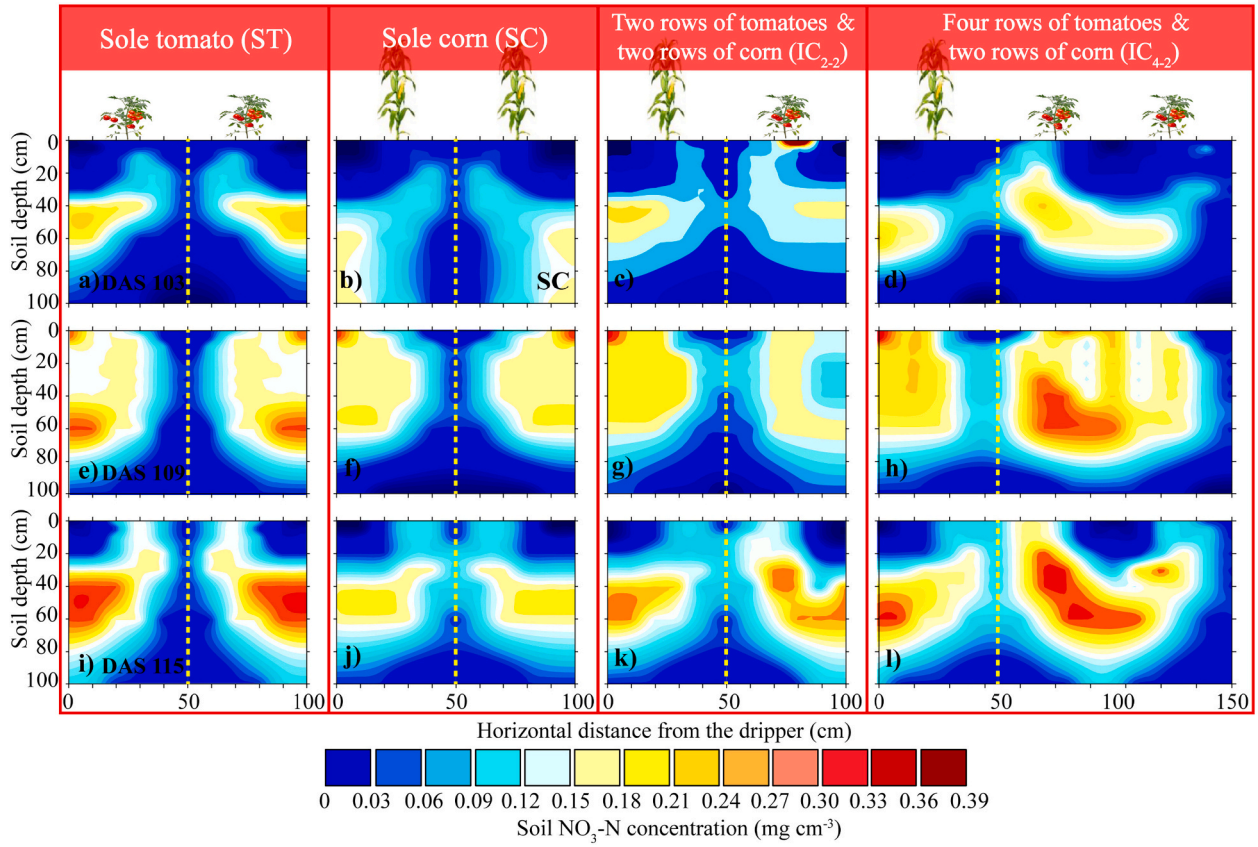

Fig. 6. Simulated two-dimensional distributions of NO_3-N concentrations one day (DAS 103) (top), seven days (DAS 109) (middle), and fourteen days (DAS 115) (bottom) after the nitrogen fertilizer application in the ST (a, e, i), SC (b, f, j), IC_{2-2} (c, g, k), and IC_{4-2} (d, h, l) systems.

cm^{-3}, respectively.

3.2. Soil nitrogen distribution in the soil profile under different intercropping systems

Since soil nitrogen distributions were similar in 2018 and 2019, only the soil nitrogen distribution in 2018 is shown (Figs. 5, 6). Additionally, soil nitrogen concentrations in the soil profile were divided into three zones, i.e., a low concentration zone (0–0.25 mg cm^{-3} for NH_4-N; 0–0.15 mg cm^{-3} for NO_3-N, LCZ), a moderate concentration zone (0.26–0.50 mg cm^{-3} for NH_4-N; 0.16–0.30 mg cm^{-3} for NO_3-N, MCZ), and a high concentration zone (>0.50 mg cm^{-3} for NH_4-N; >0.30 mg cm^{-3} for NO_3-N, HCZ).

On DAS 103, soil NH_4-N was mainly distributed in the 0–40 cm soil layer in different systems. Meanwhile, there were apparent differences in soil NH_4-N distributions between intercropping and sole-crop systems, especially for IC_{2-2} (Fig. 5). The HCZ in the root zone of tomatoes in IC_{2-2} was 31.2% and 8.5% lower than in ST and IC_{4-2}, respectively. The HCZ in the root zone of corn in IC_{2-2} increased by 47.4% and 10.4% compared with SC and IC_{4-2}, respectively. Differences in soil NH_4-N distributions among different systems on DAS 109 were lower than on DAS 103. On DAS 115, there was nearly no soil NH_4-N in the soil profile, which indicated that soil NH_4-N fully transformed into soil NO_3-N by nitrification.

Soil NO_3-N, which was present mainly in the 40–60 cm soil layer (Fig. 6), was distributed more widely (due to the lack of retardation) than soil NH_4-N. On DAS 103, no HCZ occurred under any systems, except for IC_{2-2}. The MCZ in the root zone of tomatoes in IC_{2-2} and IC_{4-2} decreased by 38.8% and 23.9% compared with ST, respectively. However, the MCZ in the root zone of corn in IC_{2-2} and IC_{4-2} increased by 26.8% and 33.5% compared with SC, respectively. The LCZ in the root zone of corn in IC_{2-2} and IC_{4-2} decreased by 5.4% and 3.3% compared with SC, respectively. The MCZ under different systems increased on DAS 109. The MCZ in the root zone of tomatoes in IC_{2-2} and IC_{4-2} decreased by 18.2% and 4.1% compared with ST, respectively. The MCZ in the root zone of corn in IC_{2-2} and IC_{4-2} was 40.2% and 33.0% higher than in SC, respectively. On DAS 115, when nitrification of NH_4-N to NO_3-N was practically over, the differences in soil NO_3-N distributions among ST, SC, IC_{2-2}, and IC_{4-2} were the highest (Fig. 6). The HCZ in the root zone of tomatoes in IC_{2-2} and IC_{4-2} was 28.5% and 16.1% lower than in ST, respectively. The MCZ and LCZ in the root zone of tomatoes in IC_{2-2} increased by 12.2% and 14.3% compared with ST, respectively, while it was 5.8% and 2.8% higher in IC_{4-2}. Additionally, the HCZ in the root zone of corn only occurred in IC_{2-2} and IC_{4-2}. The MCZ and LCZ in the root zone of corn in IC_{2-2} decreased by 26.2% and 9.4% compared with SC, respectively, while it was 57.0% and 5.5% lower in IC_{4-2}.

3.3. Exchange of soil nitrogen between the root zones of tomatoes and corn in different intercropping systems

A hypothetical vertical line 50 cm away from the dripper (Fig. 1) was defined to capture the nature of nitrogen competition between intercropping species in different intercropping systems. The left and right regions on two sides of the hypothetical vertical line were denoted as “Region I" and “Region II,” respectively. The nitrogen flux between Regions I (i.e., the root zone of corn in the intercropping system) and II (i.e., the root zone of tomatoes in the intercropping system) across this vertical line was calculated.

The highest inter-species competition for nitrogen between tomatoes and corn occurred during the second stage (DAS 41–120) (Fig. 7). Moreover, the largest nitrogen flux occurred in the IC_{2-2} system. The average nitrogen flux in IC_{2-2} during the second stage in 2018 increased

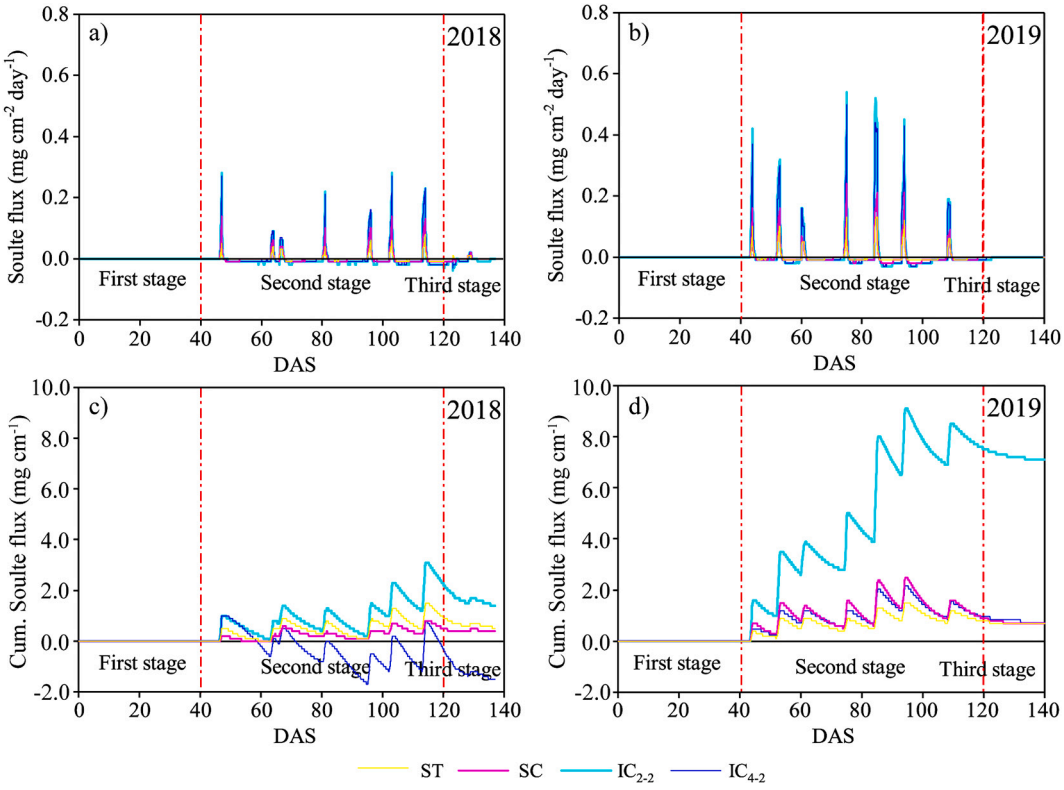

Fig. 7. Simulated actual (top) and cumulative (bottom) soil nitrogen fluxes in 2018 (left) and 2019 (right) in the horizontal direction between regions I and II (at a vertical line 50 cm away from the dripper) in the ST, SC, IC_{2-2}, and IC_{4-2} systems. Note that regions I and II represent the root zone of corn and tomatoes in the intercropping system, respectively.

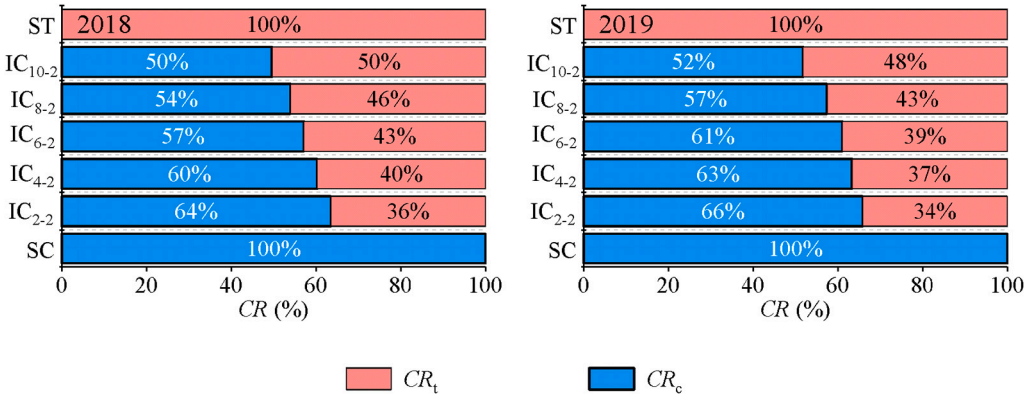

Fig. 8. The simulated competitive ratios for nitrogen for tomatoes (CR_t) and corn (CR_c) in the ST, SC, IC_{2-2}, IC_{4-2}, IC_{6-2}, IC_{8-2}, and IC_{10-2} systems in 2018 (left) and 2019 (right).

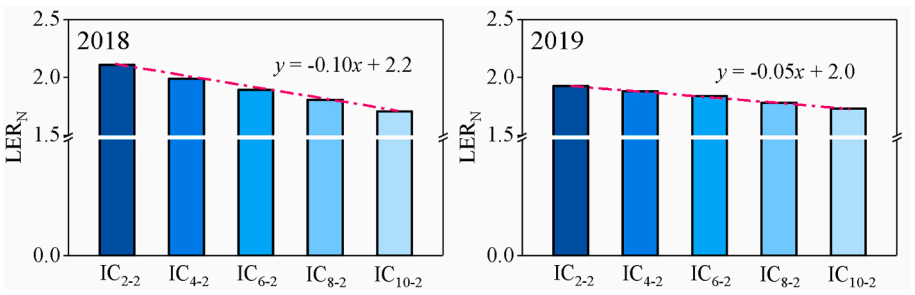

Fig. 9. The simulated land equivalent ratios for nitrogen (LER_N) between tomatoes and corn in the IC_{2-2}, IC_{4-2}, IC_{6-2},IC_{8-2}, and IC_{10-2} systems in 2018 (left) and 2019 (right).

Table 2
Statistical results for simulated soil NH_4-N and NO_3-N concentrations in the middle of two corn rows (P_c) and two tomato rows (P_t) in the systems with sole tomato (ST), sole corn (SC), two rows of tomatoes intercropping two rows of corn (IC_{2-2}), and four rows of tomatoes intercropping two rows of corn (IC_{4-2}) during calibration (2018) and validation (2019). *PBIAS*, *IA*, and *nRMSE* are the percent bias, the index of agreement, and the normalized root mean square error, respectively.

Year			Soil layers (cm)	ST			SC			IC_{2-2}			IC_{4-2}		
				PBIAS (%)	*IA* (−)	*nRMSE* (%)	*PBIAS* (%)	*IA* (−)	*nRMSE* (%)	*PBIAS* (%)	*IA* (−)	*nRMSE* (%)	*PBIAS* (%)	*IA* (−)	*nRMSE* (%)
2018	NH_4-N	P_c	0–20				7.4	0.92	7.1	9.6	0.88	5.1	−7.6	0.94	7.4
			20–40				8.1	0.90	6.3	8.7	0.84	7.7	−8.4	0.87	8.9
			40–100				−9.3	0.87	8.7	10.9	0.80	9.1	−9.7	0.82	7.9
		P_t	0–20	7.7	0.93	5.4				10.8	0.86	9.8	7.5	0.94	6.2
			20–40	−7.0	0.93	5.7				−9.0	0.86	7.4	−8.0	0.85	6.8
			40–100	8.5	0.90	6.2				8.3	0.87	6.1	8.6	0.86	7.9
	NO_3-N	P_c	0–20				−10.1	0.86	8.5	−7.1	0.93	5.6	6.4	0.93	5.7
			20–40				9.4	0.86	6.9	−10.8	0.80	7.3	−7.8	0.96	8.2
			40–100				−8.8	0.89	6.5	−5.2	0.97	2.8	5.6	0.96	5.5
		P_t	0–20	−9.9	0.86	7.7				−9.9	0.84	8.0	10.0	0.87	9.0
			20–40	−8.1	0.90	6.1				−8.2	0.88	10.4	−9.4	0.93	9.0
			40–100	7.2	0.92	5.4				7.8	0.91	6.6	10.1	0.78	11.1
2019	NH_4-N	P_c	0–20				−8.4	0.90	7.8	10.8	0.84	8.0	12.1	0.77	11.5
			20–40				9.5	0.86	8.7	10.0	0.83	7.9	9.2	0.89	6.8
			40–100				10.6	0.84	9.2	9.5	0.86	5.3	8.8	0.91	8.1
		P_t	0–20	9.6	0.84	7.7				11.9	0.85	9.6	11.0	0.82	7.6
			20–40	11.9	0.98	10.6				11.6	0.88	7.7	9.1	0.83	6.0
			40–100	9.3	0.96	11.4				−8.8	0.91	10.2	9.2	0.83	10.0
	NO_3-N	P_c	0–20				12.6	0.84	8.6	11.0	0.84	9.8	9.4	0.84	6.4
			20–40				11.1	0.81	8.8	12.0	0.84	8.7	13.5	0.72	8.9
			40–100				9.5	0.82	4.1	6.3	0.97	3.7	−9.9	0.79	7.1
		P_t	0–20	12.4	0.82	8.2				10.7	0.81	8.9	9.0	0.79	7.6
			20–40	9.4	0.94	6.3				9.5	0.88	8.4	4.5	0.99	6.0
			40–100	8.6	0.86	7.4				9.2	0.89	8.3	−13.3	0.75	12.4

by 76.7%, 47.4%, and 5.8% compared with ST, SC, and IC_{4-2}, respectively, while in 2019, it increased by 69.4%, 50.0%, and 5.7%, respectively. The highest cumulative nitrogen flux among different systems occurred in IC_{2-2}. The average cumulative nitrogen flux in IC_{2-2} in 2018 was 64.3%, 71.4%, and 207.1% higher than in ST, SC, and IC_{4-2}, respectively, and the corresponding values in 2019 were 90.1%, 87.2%, and 89.6% higher. IC_{2-2} had the highest actual and cumulative nitrogen fluxes among all systems.

3.4. Soil nitrogen balance and nitrogen use efficiency

Inter-species nitrogen competition resulted in apparent differences in the soil nitrogen balance in the root zone of corn and tomatoes of different intercropping systems. In general, IC_{4-2} had higher nitrogen leaching than IC_{2-2} and ST from the root zones of corn and tomatoes, respectively (Table 3). Nitrogen leaching from the corn root zone in IC_{4-2} increased by 39.4% compared with IC_{2-2}. Furthermore, nitrogen leaching from the root zone of tomatoes in IC_{4-2} increased by 72.9% compared with ST. However, the highest total nitrogen uptake (i.e., the sum of nitrogen uptake by corn and tomatoes) occurred in the IC_{2-2} system, with an average of 241.1 kg ha^{-1} in both years. Simulated corn nitrogen uptake in IC_{2-2} was 16.3% and 9.1% higher than in SC and IC_{4-2}, respectively. Tomato nitrogen uptake in IC_{2-2} was 9.1% and 2.8% lower than in ST and IC_{4-2}, respectively. Meanwhile, the simulation accuracy of crop nitrogen uptake is high, with the mean relative error of only 6.3% and 7.4% for corn and tomatoes, respectively (Table 3). The nitrogen storage in IC_{4-2} was apparently higher than in other treatments, except for ST. The average nitrogen storage in the root zone of corn in IC_{4-2} increased by 16.4% and 8.8% compared with SC and IC_{2-2}, respectively. The average nitrogen storage in the root zone of tomatoes in IC_{4-2} was 1.6% higher than in IC_{2-2}, while it was 2.6% lower than in ST. However, corn biomass was highest in IC_{2-2}, with an average of 29.2 t ha^{-1} in both years, 11.1% and 5.3% higher than in SC and IC_{4-2}, respectively. Among different intercropping systems, the highest tomato yield occurred in IC_{4-2}, with an average of 130.7 t ha^{-1} in both years. Also, corn yield was highest in IC_{2-2}, with an average of 13.4 t ha^{-1} in both years, 14.1% and 5.9% higher than in SC and IC_{4-2}, respectively. Among different intercropping systems, the highest tomato yield occurred in IC_{4-2}, with an average of 98.8 t ha^{-1} in both years, 18.9% higher than in IC_{2-2} ($P < 0.05$). The highest *NUE* of corn and tomatoes occurred in IC_{2-2} and ST, respectively (Table 3). *NUE* of corn in IC_{2-2} was 14.1% and 5.6% higher than in SC and IC_{4-2}, respectively. *NUE* of tomato in ST was 23.5% and 5.8% higher than in IC_{2-2} and IC_{4-2}, respectively. However, the highest LER_{NUE} occurred in IC_{4-2}, with an average of 2.0 in both years, and it increased by 5.4% compared with IC_{2-2} ($P > 0.05$). Therefore, IC_{4-2} was better than IC_{2-2} in terms of LER_{NUE} for the intercropping system.

3.5. Soil nitrogen competition between corn and tomatoes in different intercropping systems

The result of these scenario simulations showed that the competitive ratio for nitrogen by corn (CR_c) decreased by 5.3% and 4.4% in 2018 and 2019, respectively, with an increase in the planting ratio of tomatoes, while the competitive ratio for nitrogen by tomatoes (CR_t) increased by 7.4% and 7.1%, respectively (Fig. 8). Additionally, the highest LER_N occurred in the IC_{2-2} system, with an average of 2.0 in both years. With an increase in the planting ratio of tomatoes, LER_N of the tomato-corn intercropping system decreased by 12.4% and 6.1%, respectively (Fig. 9).

3.6. Economic benefit analysis of different intercropping systems

Large differences in the economic benefits of different cropping systems were found due to different crop yields (Table 4). In general, investment (*TI*) increased in response to an increase in the planting ratio of tomatoes. The highest *TI* (among different intercropping systems) occurred in the IC_{4-2} system, with a two-year average of 4839.3 $ ha^{-1}, which was 63.5% and 16.7% higher than for the SC and IC_{2-2} systems, respectively. However, *TI* of the IC_{4-2} system decreased by 18.5% compared with the ST system. Additionally, the IC_{4-2} system had the highest total revenue (*TR*) among different systems. *TR* of the IC_{4-2} system was 37.9%, 60.1%, and 7.6% higher in 2018 and 42.9%, 60.7%, and 8.6% higher in 2019 than for the ST, SC, and IC_{2-2} systems,

Table 3
Simulated soil nitrogen balance, observed crop nitrogen uptake (CNU), biomass, crop yield (*Y*), uptake efficiency (*UE*), physiological efficiency (*PE*), nitrogen use efficiency (*NUE*), and the land equivalent ratio for nitrogen use efficiency (LER_{NUE}) for corn and tomatoes in the systems with sole tomato (ST), sole corn (SC), two rows of omatoes intercropping two rows of corn (IC_{2-2}), and four rows of tomatoes intercropping two rows of corn (IC_{4-2}) during the 2018 and 2019 seasons.

Year	Treatment	Simulated nitrogen balance (kg ha^{-1})								CNU (kg ha^{-1})		Biomass (t ha^{-1})		*Y* (t ha^{-1})		*UE*		*PE*		*NUE*		LER_{NUE}
		Applied		Leached		Uptaken		Stored														
		Corn	Tomato	Corn	Tomato	Corn	Tomato	Corn	Tomato	Corn	Tomato	Corn	Tomato	Corn	Tomato	Corn	Tomato	Corn	Tomato	Corn	Tomato	
2018	ST	–	150	–	3.7	–	103.7	–	42.6	–	115.2a	–	152.2a	–	120.2a	–	0.8a	–	1043.4a	–	801.3a	–
	SC	210	–	47.7	–	137.5	–	24.8	–	125.4c	–	28.4c	–	12.8c	–	0.6b	–	102.1a	–	61.0bc	–	–
	IC_{2-2}	210	150	16.9	14.5	164.6	94.6	28.5	40.9	172.5a	89.7c	32.0a	119.5b	14.8a	89.6b	0.8a	0.6b	85.8b	998.9ab	70.5a	597.3c	1.9b
	IC_{4-2}	210	150	32.9	12.7	145.7	96.1	31.4	41.2	153.7b	102.4b	29.2b	147.6a	13.5b	112.2a	0.7ab	0.7ab	87.8b	1095.7a	64.3ab	748.0b	2.0ab
2019	ST	–	150	–	1.8	–	84	–	64.2	–	92.5c	–	117.6b	–	89.4b	–	0.6b	–	966.5b	–	596.0c	–
	SC	210	–	41.6	–	123.2	–	45.2	–	112.8d	–	23.6e	–	10.2e	–	0.5c	–	90.4b	–	48.6d	–	–
	IC_{2-2}	210	150	15.4	12.5	146.8	76.1	47.8	61.4	153.2b	82.1d	26.4d	94.3c	12.0d	70.7c	0.7ab	0.5c	78.3c	861.1c	57.1c	471.3d	2.0ab
	IC_{4-2}	210	150	20.4	7.6	137.3	79.6	52.3	62.8	130.6c	84.8d	26.1d	113.7b	11.8d	85.3b	0.6b	0.6b	90.4b	1005.9a	56.2c	568.7c	2.1a

respectively. Overall, the highest net revenue (*NR*) occurred in the IC_{4-2} system, with an average of 8221.0 $ ha^{-1}, which was 77.1%, 58.5%, and 2.9% higher than for the ST, SC, and IC_{2-2} systems, respectively (Table 4). Therefore, IC_{4-2} can be recommended as the optimal system to increase farmer's income.

4. Discussion

4.1. Soil nitrogen distribution in the soil profile of the tomato-corn intercropping system

Differences in soil NH_4-N distributions in the crop root zone are primarily affected by the difference in the nitrogen fertilizer application amounts and root nitrogen uptake (Dittrich et al., 2021). For example, the soil NH_4-N concentrations in the root zone of corn in the IC_{2-2} and IC_{4-2} systems increased by 12.4% and 3.2% compared with the root zone of tomatoes, respectively (Fig. 3). The causes of this phenomenon are manifold. On the one hand, the application of nitrogen fertilizer for corn was higher than for tomatoes, which resulted in high soil NH_4-N concentrations occurring in the root zone of corn after fertilization. On the other hand, the ability of corn roots to uptake soil NH_4-N was low, causing soil NH_4-N to accumulate in the corn root zone (Giles et al., 2017; Livesley et al., 2002). The variation of the planting ratio of interspecies in different intercropping systems would change the soil profile's nitrogen distribution. For example, the highest soil NH_4-N concentration in P_c occurred in the SC system among different systems (Fig. 3). The cause of this phenomenon is that the SC system has the highest planting ratio of corn. Moreover, the ability of corn roots to uptake soil NH_4-N was low. Therefore, more soil NH_4-N was accumulated in the corn root zone in the SC system compared with the IC_{2-2} and IC_{4-2} systems. However, the highest soil NH_4-N concentrations in P_t occurred in the IC_{2-2} system among different systems. Since the ability of tomato roots to uptake soil NH_4-N was higher than that of corn roots, soil NH_4-N concentrations in the soil profile increased in response to a decrease in the planting ratio of tomatoes. Thus, soil NH_4-N concentrations in P_t in the IC_{2-2} system were higher than in the ST and IC_{4-2} systems.

Additionally, soil NH_4-N in the soil profile of the tomato-corn intercropping system is mainly distributed in the top 0–40 cm soil layer. The main reason is that soil particles easily adsorb soil NH_4-N after being hydrolyzed from urea (Kothawala and Moore, 2009; Sasaki et al., 2002; Teutscherova et al., 2018). Furthermore, the fast nitrification rate of soil NH_4-N limited its redistribution in the soil profile. Al-Wabel (2019) indicated that soil NH_4-N concentrations significantly decreased 15 days after fertilization, while soil NO_3-N concentrations increased considerably. This study similarly found that soil NH_4-N was fully nitrified into soil NO_3-N 12 days after fertilization.

Heterogeneous distribution of soil NO_3-N was found in the tomato-corn intercropping system. In general, soil NO_3-N concentrations in the root zone of tomatoes were higher than in the root zone of corn (Chen et al., 2020a). The reason may be attributed to the better ability of corn roots to uptake nitrate compared with tomatoes (Reed and Hageman, 1980). Although a high amount of NH_4-N accumulated in the root zone of corn promoted nitrification, soil NO_3-N concentrations in the root zone of corn significantly decreased due to intensive root uptake of corn. For example, this study found that soil NO_3-N concentrations in the root zone of corn in the IC_{2-2} and IC_{4-2} systems decreased by 31.5% and 22.9% compared with the root zone of tomatoes, respectively (Fig. 4). Nevertheless, soil NO_3-N concentrations in the root zone of corn in the IC_{4-2} system were higher than in the SC and IC_{2-2} systems. This can be attributed to the difference in the planting ratio of the dominant species (i.e., corn) in different intercropping systems. A high planting ratio of corn would significantly decrease soil NO_3-N concentrations in the root zone due to its high ability to uptake nitrate. In contrast, a high planting ratio of tomatoes would increase soil NO_3-N concentrations in the root zone due to their weak ability to uptake nitrate, e.g., soil NO_3-N concentrations in the root zone of tomatoes in the ST system were higher

Table 4
Crop yields (*Y*), investments (*I*), revenues (*R*), total investments (*TI*), total revenues (*TR*), and net revenues (*NR*) of corn and tomatoes in the systems with sole tomatoes (ST), sole corn (SC), two rows of tomatoes intercropping two rows of corn (IC_{2-2}), and four rows of tomatoes intercropping two rows of corn (IC_{4-2}) during the 2018 and 2019 seasons. Different letters in the same column indicate a significant difference ($P < 0.05$) among treatments.

Year	Treatment	Crop	*Y* (t ha^{-1})	*I* ($ ha^{-1})	*R* ($ ha^{-1})	*TI* ($ ha^{-1})	*TR* ($ ha^{-1})	*NR* ($ ha^{-1})
2018	ST	Corn	–	–	–	5952.4	8968.1e	3015.8d
		Tomato	120.2a	5952.4	8968.1a			
	SC	Corn	12.8f	1786.4	5760.0f	1786.4	5760.0 g	3973.6c
		Tomato	–	–	–			
	IC_{2-2}	Corn	14.8d	767.0	6660.0c	4033.4	13,345.1b	9311.6a
		Tomato	89.6b	3266.4	6685.1c			
	IC_{4-2}	Corn	13.5e	575.0	6075.0e	4842.4	14,446.2a	9603.9a
		Tomato	112.2a	4267.3	8371.2b			
2019	ST	Corn	–	–	–	5919.7	6670.1f	750.4e
		Tomato	89.4b	5919.7	6670.1c			
	SC	Corn	10.2 h	1743.9	4590.0 h	1743.9	4590.0 h	2846.1d
		Tomato	–	–	–			
	IC_{2-2}	Corn	12.0 g	763.9	5400.0 g	4027.2	10,674.9d	6647.7b
		Tomato	70.7c	3263.3	5274.9 g			
	IC_{4-2}	Corn	11.8 g	571.9	5310.0 g	4836.2	11,674.2c	6838.1b
		Tomato	85.3b	4264.2	6364.2d			

than in the IC_{2-2} and IC_{4-2} systems.

The mobility of soil NO_3-N promoted the redistribution of soil NO_3-N in the soil profile (Arauzo et al., 2022; Rath et al., 2021; Zilio et al., 2020). Soil NO_3-N was, in this study, accumulated mainly in the 0–80 cm soil layer of different intercropping systems (Fig. 6). Ranjbar et al. (2019) similarly indicated that soil NO_3-N was distributed in the 0–60 cm soil layer after fertilization. However, a deeper accumulation zone for soil NO_3-N was found in the previous literature (Izsaki and Ivanyi, 2002). These differences may be attributed to different irrigation strategies. For example, surface irrigation with a high flow may have resulted in soil NO_3-N leaching below the crop root zone in some of these studies. Drip irrigation with a low flow rate, which is beneficial for soil NO_3-N to storage in the crop root zone, was adapted in this study.

4.2. Nitrogen use efficiency for different intercropping systems

Variations in the planting structure caused apparent differences in crop nitrogen uptake among different systems. In general, the difference in crop nitrogen uptake among different systems increased in response to an increase in the planting ratio of dominant species (Choudhary et al., 2014; Moghbeli et al., 2019; Neugschwandtner and Kaul, 2015). For instance, Salehi et al. (2018) showed that the highest crop nitrogen uptake occurred in the IC_{2-2} system involving fenugreek and buckwheat, and nitrogen uptake decreased with an increasing share of buckwheat. This study similarly found that corn nitrogen uptake in the IC_{2-2} system was 16.3% higher than in SC, and tomato nitrogen uptake was 9.1% lower than in ST. The reason for this is the higher ability of corn to uptake nitrogen compared with tomatoes (Chen et al., 2020a), i.e., the competition mechanism increased the physiological nitrogen content of corn.

Although total nitrogen uptake in the intercropping system can be improved by increasing the planting ratio of dominant species, the unreasonable planting structure will break the competitive nitrogen balance for inter-species. For example, the cumulative solute flux in IC_{2-2} was 77.2% and 79.3% higher than in ST and SC, respectively (Fig. 7). The main reason is that the IC_{2-2} system has the larger horizontal solute gradient between the root zones of tomatoes and corn, especially during the rapid crop growth stage (i.e., the second stage). However, the cumulative solute flux in the IC_{4-2} system remained near zero, which indicated that the nitrogen inter-specific competition between tomatoes and corn reached a relative balance.

Additionally, the competitive ratio for nitrogen of inter-species reached a relative balance with an increase in the planting ratio of tomatoes, while LER_N of the intercropping system markedly decreased (Figs. 8 and 9). The reason is that nitrogen uptake of the intercropping system mainly depends on corn, and an excessive increase in the planting ratio of tomatoes will reduce the total nitrogen uptake of the intercropping system. However, LER_{NUE} increased in response to an increase in the planting ratio of tomatoes. For example, LER_{NUE} in the IC_{4-2} system increased by 5.4% compared with the IC_{2-2} system (Table 2). The main reason is that the *NUE* of tomatoes was higher than that of corn. Thus, *NUE* in the intercropping system can be effectively improved by reasonably increasing the planting ratio of tomatoes. The IC_{4-2} system can therefore be recommended to local farmers to increase LER_{NUE} of the intercropping system.

5. Conclusions

HYDRUS (2D/3D), modified to consider two vegetations, can precisely capture the dynamics of soil NH_4-N and NO_3-N in the tomato-corn intercropping system. The differences in soil NH_4-N among different systems occurred in the surface soil layer (0–40 cm), especially in the 0–20 cm soil layer. Soil NH_4-N concentrations at P_t and P_c of different systems decreased as follows: $IC_{2-2} > IC_{4-2} >$ ST and SC $> IC_{2-2} > IC_{4-2}$, respectively. Compared with soil NH_4-N, differences in soil NO_3-N in different systems were more evident due to the mobility of NO_3-N. Soil NO_3-N was mainly distributed in the 40–60 cm soil layer. The highest inter-species competition for nitrogen between tomatoes and corn occurred during the second stage (DAS 41–120). IC_{2-2} had the highest nitrogen flux, cumulative nitrogen flux, and nitrogen uptake among different systems. However, the highest LER_{NUE} occurred in the IC_{4-2} system, with an average of 2.0 in both years. Therefore, IC_{4-2} can be recommended to local farmlands to increase the *NUE* of intercropping systems. Moreover, with an increase in the planting ratio of tomatoes (a subordinate species), CR_t for tomatoes and LER_N for the intercropping system showed increasing and decreasing trends, respectively.

Declaration of Competing Interest

The authors declare that they have no known competing financial interests or personal relationships that could have appeared to influence the work reported in this paper.

No conflict of interest exits in the submission of this manuscript, and manuscript is approved by all authors for publication. I would like to declare on behalf of my co-authors that the work described was original research that has not been published previously, and not under consideration for publication elsewhere, in whole or in part. All the authors listed have approved the manuscript that is enclosed.

Acknowledgments

This research was jointly supported by the National Natural Science Foundation of China (51969024, 52079064 and 51669020), the Local Science and Technology Development Fund Projects Guided by the Central Government (2020ZY0023), the Trans formation Projects of Scientific and Technological Achievements of Inner Mongolia (2022YFHH0039), and the Inner Mongolia Autonomous Region Graduate Education Innovation Plan Subsidize Project. Additionally, we are sincerely appreciate the careful and precise reviews by the anonymous reviewers, editors.

Appendix A. Supplementary data

Supplementary data to this article can be found online at https://doi.org/10.1016/j.agsy.2022.103461.

References

Ahmad, A., Khan, I., Abrol, Y.P., Iqbal, M., 2008. Genotypic variation of nitrogen use efficiency in Indian mustard. Environ. Pollut. 154 (3), 462–466.
Allen, R., Pereira, L.S., Raes, D., Smith, M., 1998. Crop evapotranspiration: guidelines for computing crop requirements. In: FAO Irrigation and Drainage Paper No. 56. FAO, Rome.
Al-Wabel, M.I., 2019. A short-term effect of date palm biochars on NH_3 volatilization and N transformation in calcareous sandy loam soil. Arab. J. Geosci. 12 (12).
Arauzo, M., Valladolid, M., García, G., Andries, D.M., 2022. N and P behaviour in alluvial aquifers and in the soil solution of their catchment areas: how land use and the physical environment contribute to diffuse pollution. Sci. Total Environ. 804, 150056.
Bremner, J., Keeney, D., 1965. Steam distillation methods for determination of ammonium, nitrate and nitrite. Anal. Chim. Acta 32, 485–495.
Chen, N., Li, X.Y., Šimůnek, J., Shi, H.B., Hu, Q., Zhang, Y.H., 2020a. Evaluating soil nitrate dynamics in an intercropping dripped ecosystem using HYDRUS-2D. Sci. Total Environ. 137314.
Chen, N., Li, X.Y., Šimůnek, J., Shi, H.B., Ding, Z.J., Zhang, Y.H., 2020b. The effects of biodegradable and plastic film mulching on nitrogen uptake, distribution, and leaching in a drip-irrigated sandy field. Agric. Ecosyst. Environ. 292, 106817.
Chen, N., Li, X.Y., Shi, H.B., Hu, Q., Zhang, Y.H., Hou, C.L., Liu, Y.H., 2022. Modeling evapotranspiration and evaporation in corn/tomato intercropping ecosystem using a modified ERIN model considering plastic film mulching. Agric. Water Manag. 260, 107286.
Choudhary, V.K., Choudhury, B.U., 2016. A staggered maize-legume intercrop arrangement influences yield, weed smothering and nutrient balance in the eastern Himalayan region of India. Exp. Agric. 54 (02), 181–200.
Choudhary, V.K., Dixit, A., Kumar, P.S., 2014. Productivity, competition behaviour and weed dynamics of various row proportions of maize (*zea mays*)-legumes intercropping in Arunachal Pradesh. Indian J. Agric. Sci. 84 (11), 1329–1334.
Coll, L., Cerrudo, A., Rizzalli, R., Monzon, J.P., Andrade, F.H., 2012. Capture and use of water and radiation in summer intercrops in the south-east pampas of Argentina. Field Crop Res. 134, 105–113.
Cote, C., Bristow, K., Charlesworth, P., Cook, F., Charlesworth, P., 2003. Analysis of soil wetting and solute transport in subsurface trickle irrigation. Irrig. Sci. 22 (3–4), 143–156.
Cruz, I.L., Aguilar, A.R., Raquel, S.M., L'opez, R.L., 2014. Global sensitivity analysis of crop growth SUCROS model applied to husk tomato. Rev. Fitotec. Mex. Publ. 37 (3), 279–288.
Daryanto, S., Fu, B., Zhao, W., Wang, S., Jacinthe, P.A., Wang, L., 2020. Ecosystem service provision of grain legume and cereal intercropping in Africa. Agric. Syst. 178, 102761.
De Conti, L., Ceretta, C.A., Melo, G.W.B., Tiecher, T.L., Silva, L.O.S., Garlet, L.P., Mimmo, T., Cesco, S., Brunetto, G., 2019. Intercropping of young grapevines with native grasses for phytoremediation of cu-contaminated soils. Chemosphere 216, 147–156.
Dittrich, F., Iserloh, T., Treseler, C.-H., Hüppi, R., Ogan, S., Seeger, M., Thiele-Bruhn, S., 2021. Crop diversification in viticulture with aromatic plants: effects of intercropping on grapevine productivity in a steep-slope vineyard in the Mosel area, Germany. Agriculture 11 (2), 95.
Drakopoulos, D., Kägi, A., Six, J., Zorn, A., Wettstein, F.E., Bucheli, T.D., Rudolf Forrer, H., Vogelgsang, S., 2021. The agronomic and economic viability of innovative cropping systems to reduce Fusarium head blight and related mycotoxins in wheat. Agric. Syst. 192, 103198.
Dua, V.K., Kumar, S., Jatav, M.K., 2016. Effect of nitrogen application to intercrops on yield, competition, nutrient use efficiency and economics in potato (solanum tuberosum l.) + french bean (phaseolus vulgaris l.) system in north-western hills of India. Legum. Res. 40 (4), 698–703.
Feddes, R., Kowalik, P., Zaradny, H., 1978. Simulation of Field Water Use and Crop Yield. John Wiley & Sons, New York.
Fernandez, J.A., Habben, J.E., Schussler, J.R., Masek, T., Weers, B., Bing, J., Ciampitti, I. A., 2022. Zmm28transgenic maize increases both n uptake- and n utilization-efficiencies. Commun. Biol. 5, 555.
Filipovic, V., Coquet, Y., Pot, V., Houot, S., Benoit, P., 2014. Modeling the effect of soil structure on water flow and isoproturon dynamics in an agricultural field receiving repeated urban waste compost application. Sci. Total Environ. 499, 546–559.
Firouzi, S., Nikkhah, A., Rosentrater, K.A., 2017. An integrated analysis of non-renewable energy use, GHG emissions, carbon efficiency of groundnut sole cropping and groundnut-bean intercropping agro-ecosystems. Environ. Prog. Sustain. Energy 36 (6), 1832–1839.
Galanopoulou, K., Lithourgidis, A.S., Dordas, C.A., 2019. Intercropping of faba bean with barley at various spatial arrangements affects dry matter and N yield, nitrogen nutrition index, and interspecific competition. Not. Bot. Horti Agrobot. Cluj-Napoca 47 (4), 1116–1127.
Gao, R., Guo, G., Fang, C., Huang, S., Chen, J., Lu, R., Huang, J., Fan, X., Liu, C., 2018. Rapid generation of barley mutant lines with high nitrogen uptake efficiency by microspore mutagenesis and field screening. Front. Plant Sci. 9, 450.
Gaudinier, A., Rodriguez-Medina, J., Zhang, L., Olson, A., Liseron-Monfils, C., Bågman, A.M., Foret, J., Abbitt, S., Tang, M., Li, B.H., Runcie, D.E., Kliebenstein, D. J., Shen, B., Frank, M.J., Ware, D., Brady, S.M., 2018. Transcriptional regulation of nitrogen-associated metabolism and growth. Nature. 563 (7730), 259.
Ghosh, P.K., Tripathi, A.K., Bandyopadhyay, K.K., Manna, M.C., 2009. Assessment of nutrient competition and nutrient requirement in soybean/sorghum intercropping system. Eur. J. Agron. 31 (1), 43–50.
Giles, C.D., Brown, L.K., Adu, M.O., Mezeli, M.M., Sandral, G.A., Simpson, R.J., Wendler, R., Shand, C.A., Menezes-Blackburn, D., Darch, T., Stutter, M.I., Lumsdon, D.G., Zhang, H., Blackwell, M.S.A., Wearing, C., Cooper, P., Haygarth, P. M., George, T.S., 2017. Response-based selection of barley cultivars and legume species for complementarity: root morphology and exudation in relation to nutrient source. Plant Sci. 255, 12–28.
Gitari, H.I., Nyawade, S.O., Kamau, S., Karanja, N.N., Gachene, C.K.K., Raza, M.A., Maitra, S., Schulte-Geldermann, E., 2020. Revisiting intercropping indices with respect to potato-legume intercropping systems. Field Crop Res. 258, 107957.
Grecco, K.L., de Miranda, J.H., Silveira, L.K., van Genuchten, M.T, 2019. HYDRUS-2D simulations of water and potassium movement in drip irrigated tropical soil container cultivated with sugarcane. Agric. Water Manage. 221, 334–347.
Groenveld, T., Argaman, A., Šimůnek, J., Lazarovitch, N., 2021. Numerical modeling to optimize nitrogen fertigation with consideration of transient drought and nitrogen stress. Agric. Water Manag. 254, 106971.
Hajari, E., Snyman, S.J., Watt, M.P., 2016. The effect of form and level of inorganic N on nitrogen use efficiency of sugarcane grown in pots. J. Plant Nutr. 40 (2), 248–257.
Hanson, B., Šimůnek, J., Hopmans, J., 2006. Evaluation of urea–ammonium–nitrate fertigation with drip irrigation using numerical modeling. Agric. Water Manag. 86 (1–2), 102–113.
Izsaki, Z., Ivanyi, I., 2002. Effect of N fertilizer on the nitrogen balance of the soil and on NO_3-N leaching in a long-term mineral fertilization experiment. Int. J. Syst. Sci. 51 (1), 115–124.
Jensen, E.S., Chongtham, I.R., Dhamala, N.R., Rodriguez, C., Carlsson, G., 2020. Diversifying European agricultural systems by intercropping. Int. J. Agr. Nat. Res. 47 (3), 174–186.
Kothawala, D.N., Moore, T.R., 2009. Adsorption of dissolved nitrogen by forest mineral soils. Can. J. For. Res. 39 (12), 2381–2390.
Latati, M., Dokukin, P., Aouiche, A., Rebouh, N.Y., Takouachet, R., Hafnaoui, E., Hamdani, F.Z., Bacha, F., Ounane, S.M., 2019. Species interactions improve above-ground biomass and land use efficiency in intercropped wheat and chickpea under low soil inputs. Agronomy 9 (11), 765.
Li, L., 2016. Intercropping enhances agroecosystem services and functioning: Current knowledge and perspectives. Chin. J. Eco-Agric. 24 (4), 403–415.
Li, X.Y., Shi, H.B., Šimůnek, J., Gong, X.W., Peng, Z.Y., 2015. Modeling soil water dynamics in a drip-irrigated intercropping field under plastic mulch. Irrig. Sci. 33 (4), 289–302.
Li, Y., Šimůnek, J., Jing, L., Zhang, Z., Ni, L., 2014. Evaluation of water movement and water losses in a direct-seeded-rice field experiment using Hydrus-1D. Agric. Water Manag. 142, 38–46.
Li, J., Xie, R.Z., Wang, K.R., Hou, P., Ming, B., Zhang, G.Q., Ming, B., Zhang, G.Q., Liu, G. Z., Wu, M., Yang, Z.S., Li, S.K., 2018. Response of canopy structure, light interception and grain yield to plant density in maize. J. Agric. Sci. 156 (6), 785–794.
Liu, Y.X., Zhang, W.P., Sun, J.H., Li, X.F., Christie, P., Li, L., 2015. High morphological and physiological plasticity of wheat roots is conducive to higher competitive ability of wheat than maize in intercropping systems. Plant Soil 397 (1–2), 387–399.
Livesley, S.J., Gregory, P.J., Buresh, R.J., 2002. Competition in tree row agroforestry systems. 2. Distribution, dynamics and uptake of soil inorganic n. Plant Soil 247 (2), 177–187.
Long, G., Li, L., Wang, D., Zhao, P., Tang, L., Zhou, Y., Yin, X., 2021. Nitrogen levels regulate intercropping-related mitigation of potential nitrate leaching. Agric. Ecosyst. Environ. 319, 107540.
Maitra, S., Hossain, A., Brestic, M., Skalicky, M., Ondrisik, P., Gitari, H., Brahmachari, K., Shankar, T., Bhadra, P., Palai, J.B., Jena, J., Bhattacharya, U., Duvvada, S.K., Lalichetti, S., Sairam, M., 2021. Intercropping—a low input agricultural strategy for food and environmental security. Agronomy 11 (2), 343.
Manevski, K., Børgesen, C.D., Andersen, M.N., Kristensen, I.S., 2014. Reduced nitrogen leaching by intercropping maize with red fescue on sandy soils in North Europe: a combined field and modeling study. Plant Soil 388 (1–2), 67–85.

Moghbeli, T., Bolandnazar, S., Panahande, J., Raei, Y., 2019. Evaluation of yield and its components on onion and fenugreek intercropping ratios in different planting densities. J. Clean. Prod. 213, 634–641.
Moll, R.H., Kamprath, E.J., Jackson, W.A., 1982. Analysis and interpretation of factors which contribute to effifficiency of nitrogen utilization. Agron. J. 74, 562e564.
Morugán-Coronado, A., Linares, C., Gómez-López, M.D., Faz, A., Zornoza, R., 2020. The impact of intercropping, tillage and fertilizer type on soil and crop yield in fruit orchards under Mediterranean conditions: a meta-analysis of field studies. Agric. Syst. 178, 102736.
Nakamura, K., Harter, T., Hirono, Y., Horino, H., Mitsuno, T., 2004. Assessment of root zone nitrogen leaching as affected by irrigation and nutrient management practices. Vadose Zone J. 3, 1353–1366.
Nassab, A.D.M., Amon, T., Kaul, H.P., 2011. Competition and yield in intercrops of maize and sunflower for biogas. Ind. Crop. Prod. 34 (1), 1203–1211.
Nelson, W.C.D., Siebrecht-Scholl, D.J., Hoffmann, M.P., Rotter, R.P., Whitbread, A.M., Link, W., 2021. What determines a productive winter bean-wheat genotype combination for intercropping in central Germany? Eur. J. Agron. 128, 126294.
Neugschwandtner, R.W., Kaul, H.P., 2015. Nitrogen uptake, use and utilization efficiency by oat–pea intercrops. Field Crop Res. 179, 113–119.
Rai, V., Pramanik, P., Das, T.K., Aggarwal, P., Bhattacharyya, R., Krishnan, P., Sehgal, V. K., 2019. Modelling soil hydrothermal regimes in pigeon pea under conservation agriculture using Hydrus-2D. Soil Tillage Res. 190, 92–108.
Ramos, T., Šimůnek, J., Gonçalves, M., Martins, J., Prazeres, A., Pereira, L., 2012. Two-dimensional modeling of water and nitrogen fate from sweet sorghum irrigated with fresh and blended saline waters. Agric. Water Manag. 111, 87–104.
Ranjbar, A., Rahimikhoob, A., Ebrahimian, H., Varavipour, M., 2019. Simulation of nitrogen uptake and distribution under furrows and ridges during the maize growth period using HYDRUS-2D. Irrig. Sci. 37 (4), 495–509.
Rath, S., Zamora-Re, M., Graham, W., Dukes, M., Kaplan, D., 2021. Quantifying nitrate leaching to groundwater from a corn-peanut rotation under a variety of irrigation and nutrient management practices in the Suwannee River basin, Florida. Agric. Water Manag. 246, 106634.
Reed, A.J., Hageman, R.H., 1980. Relationship between nitrate uptake, flux, and reduction and the accumulation of reduced nitrogen in maize (*zea mays l.*): ii. Effect of nutrient nitrate concentration. Plant Physiol. 66 (6), 1184–1189.
Salehi, A., Mehdi, B., Fallah, S., Kaul, H.P., Neugschwandtner, R.W., 2018. Productivity and nutrient use efficiency with integrated fertilization of buckwheat–fenugreek intercrops. Nutr. Cycl. Agroecosyst. 110 (3), 407–425.
Salgado, G.C., Ambrosano, E.J., Rossi, F., Otsuk, I.P., Ambrosano, G.M.B., Santana, C.A., Muraoka, T., Trivelin, P.C.O., 2021. Biological N fixation and N transfer in an intercropping system between legumes and organic cherry tomatoes in succession to green corn. Agriculture 11 (8), 690.
Sasaki, Y., Ando, H., Kakuda, K., 2002. Relationship between ammonium nitrogen in soil solution and tiller number at early growth stage of rice. Soil Sci. Plant Nutr. 48 (1), 57–63.
Šimůnek, J., van Genuchten, M.T., Šejna, M., 2016. Recent developments and applications of the HYDRUS computer software packages. Vadose Zone J. 15, 25.
Szumigalski, A.R., Van Acker, R.C., 2006. Nitrogen yield and land use efficiency in annual sole crops and intercrops. Agron. J. 98 (4), 1030.
Tafteh, A., Sepaskhah, A., 2012. Application of HYDRUS-1D model for simulating water and nitrate leaching from continuous and alternate furrow irrigated rapeseed and maize fields. Agric. Water Manag. 113, 19–29.
Teutscherova, N., Houška, J., Navas, M., Masaguer, A., Benito, M., Vazquez, E., 2018. Leaching of ammonium and nitrate from Acrisol and Calcisol amended with holm oak biochar: a column study. Geoderma 323, 136–145.
Topp, G.C., Davis, J.L., Annan, A.P., 1980. Electromagnetic determination of soil water content: measurements in coaxial transmission lines. Water Resour. Res. 16 (3), 574–582.
Unay, A., Sabanci, I., Cinar, V.M., 2021. The effect of maize (*zea mays l.*)/soybean (*glycine max (l.) merr.*) intercropping and biofertilizer (azotobacter) on yield, leaf area index and land equivalent ratio. J. Agric. Sci. Tarim Bili. 27 (1), 76–82.
United States Department of Agriculture, 2010. Keys to Soil Taxonomy. United States Departmentof Agriculture, Soil Conservation Service.
Upadhyay, K.P., Sharma, M.D., Shakya, S.M., Ortiz-Ferrara, G., Tiwari, T.P., Sharma, R. C., 2010. Performance and profitability study of baby corn and tomato intercropping. Pak. J. Agric. Sci. 47 (3), 183–193.
van Asten, P.J.A., Wairegi, L.W.I., Mukasa, D., Uringi, N.O., 2011. Agronomic and economic benefits of coffee–banana intercropping in Uganda's smallholder farming systems. Agric. Syst. 104 (4), 326–334.
Wan, J.Y., Bao, H., Peng, W.H., An, L.Y., Jiang, Q., Yang, J.M., Zhu, C., 2020. Effects of intercropping on cadmium uptake by maize and tomato. Chin. J. Biotechnol. 36 (3), 518–528.
Wesseling, J.G., Brandyk, T., 1985. Introduction of the occurrence of high groundwater levels and surface water storage in computer program SWATRE, Nota 1636. Institute for Land and Water Management Research (ICW), Wageningen, The Netherlands.
Xu, Z., Li, C., Zhang, C., Yu, Y., van der Werf, W., Zhang, F., 2020. Intercropping maize and soybean increases efficiency of land and fertilizer nitrogen use; A meta-analysis. Field Crop Res. 246, 107661.
Xu, R.X., Zhao, H.M., Liu, G.B., Li, Y., Li, S.J., Zhang, Y.J., Liu, N., Ma, L., 2022. Alfalfa and silage maize intercropping provides comparable productivity and profitability with lower environmental impacts than wheat-maize system in the North China plain. Agric. Syst. 195, 103305.
Zhang, F.S., Li, L., 2003. Using competitive and facilitative interactions in intercropping systems enhances crop productivity and nutrient-use efficiency. Plant Soil 248 (1–2), 305–312.
Zhang, W.P., Liu, G.C., Sun, J.H., Fornara, D., Zhang, L.Z., Zhang, F.F., Li, L., 2016. Temporal dynamics of nutrient uptake by neighbouring plant species: evidence from intercropping. Funct. Ecol. 31 (2), 469–479.
Zilio, M., Motta, S., Tambone, F., Scaglia, B., Boccasile, G., Squartini, A., Adani, F., 2020. The distribution of functional N-cycle related genes and ammonia and nitrate nitrogen in soil profiles fertilized with mineral and organic N fertilizer. PLoS One 15 (6), e0228364.